IEEE Access
Multidisciplinary ⋮ Rapid Review ⋮ Open Access Journal

Received 25 December 2024, accepted 8 February 2025, date of publication 17 February 2025, date of current version 21 February 2025.

Digital Object Identifier 10.1109/ACCESS.2025.3542807

RESEARCH ARTICLE

A Quantum-Enhanced Artificial Neural Network Model for Efficient Medical Image Compression

BALASUBRAMANI SUBBIYAN[1], RENJITH PRABHAVATHI NEELAKANDAN[2], KAVISANKAR LEELASANKAR[3], RAJKUMAR RAJAVEL[4], MUTHUKUMARAN MALARVEL[5], (Senior Member, IEEE), AND ACHYUT SHANKAR[6]

[1]Department of Computer Science and Engineering, Koneru Lakshmaiah Education Foundation, Vijayawada 520002, India
[2]School of Computer Science and Engineering, Vellore Institute of Technology, Chennai 600127, India
[3]Department of Computing Technologies, Faculty of Engineering and Technology, SRM Institute of Science and Technology, Kattankulathur, Tamil Nadu 603203, India
[4]School of Engineering and Technology, Department of Computer Science and Engineering, CHRIST University, Bengaluru, Karnataka 560029, India
[5]Department of Computer Science and Engineering, Aarupadai Veedu Institute of Technology, Vinayaka Mission's Research Foundation (DU), Paiyanur, Tamil Nadu 603104, India
[6]School of Computer Science Engineering and Technology, Bennett University, Greater Noida, Uttar Pradesh 201310, India

Corresponding author: Renjith Prabhavathi Neelakandan (renjith.pn@vit.ac.in)

This work was supported by the Vellore Institute of Technology, Chennai.

ABSTRACT The ability to effectively store and transmit high-resolution images such as MRI and CT scans without losing quality is critical to modernizing medical imaging. Traditional compression methods risk losing essential medical image data, which requires perfect detail for diagnosis. Quantum algorithms use superposition and entanglement to compress faster while preserving important information. This research presents a Quantum-enhanced Artificial Neural Network (QANN) model that combines quantum feature extraction with classical neural network topologies to improve image compression. Our approach consists of converting standardized classical data into quantum states, controlling these states using parameterized quantum circuits, and measuring the resulting states to produce enhanced feature vectors. The quantum-enhanced features are fed into a traditional neural network for image compression. The experimental results clearly show that our QANN framework outperforms standard models in terms of accurate reconstructed images, reduced size, and increased space-saving percentage, especially when dealing with large and complicated datasets. The QANN model demonstrates how quantum computing can significantly enhance the effectiveness of medical image processing solutions. Kaggle brain CT and MRI datasets and COVID-CXNet chest x-ray images are used. The proposed QANN model improves peak signal-to-noise ratio (PSNR) and structural similarity index (SSIM). Using quantum technology, the image size is reduced for MRI (73.3 %), X-ray (74.1%), and CT-SCAN (71.8%) to save space.

INDEX TERMS Quantum machine learning, quantum multiclass classifier, quantum feature extraction, supervised learning.

I. INTRODUCTION

The increase in the variety of datasets in industries like healthcare, finance, and environmental science has resulted in a significant growth in the use of advanced data analysis methods. The growing amount of data, also known as big data, requires advanced computational techniques to extract valuable insights and enable well-informed decision-making processes. Although efficient, conventional machine learning (ML) methods face substantial difficulties with extensive and intricate datasets. The obstacles encompass computing constraints, optimizing parameter optimization challenges, and scalability issues [1]. Conventional machine learning methods frequently encounter constraints when dealing with extensive and complex datasets, particularly in jobs that classify many classes. These limits arise from variables such as computing complexity, overfitting, and the curse of dimensionality. The latest progress in quantum computing has created new opportunities for tackling these difficulties. Quantum computing offers a promising approach to address

The associate editor coordinating the review of this manuscript and approving it for publication was Wei Huang.

these issues and opens up new possibilities for improving classification algorithms, thanks to its built-in parallelism and superposition capabilities [2]. Fig 1 illustrates the fundamental principles of Quantum Machine Learning (QML).

Modern healthcare depends on medical imaging to improve the accuracy of diagnosis and treatment planning. It helps doctors understand complex cases by enabling 3D reconstruction of anatomical components, segmentation of specific regions (such as tumors or blood arteries), and enhancing image quality. In addition, cutting-edge techniques such as real-time image analysis and AI-assisted diagnosis optimize workflows and increase the effectiveness of procedures such as image-guided surgery. In addition, medical imaging facilitates quantitative analysis by helping to measure features such as blood flow or lesion size, which are essential for tracking disease and assessing the effectiveness of treatments.

Medical image compression addresses the difficulties of storing and transmitting the vast amounts of image data produced by modalities such as CT, MRI, and X-rays. Compression enables effective archiving, faster retrieval, and seamless sharing via telemedicine and PACS systems by reducing file sizes without compromising diagnostic quality. Optimizing bandwidth utilization and reducing storage costs enables real-time applications such as surgical guidance and remote consultations. When combined, image processing and compression ensure scalable, economical solutions while maintaining the accuracy of diagnostic data in medical systems.

Quantum computing utilizes the principles of quantum physics to perform data processing and analysis tasks previously deemed unachievable using traditional computing architectures. Quantum computers, due to their superior computational efficiency, hold great potential for effectively processing and analyzing vast datasets. This work examines the combination of quantum computing and classical ML, explicitly emphasizing the creation of hybrid quantum-classical algorithms. We propose an innovative QML methodology to enhance the precision and effectiveness of supervised learning models. Our study focuses on developing a quantum-enhanced artificial neural network that uses qubits as the essential data representation and processing components, specifically designed for binary classification tasks. The results of our study indicate that QANN can achieve comparable performance to standard models while using fewer training parameters.

Quantum neural networks (QNNs) [3] merge quantum processing techniques with traditional preprocessing to enhance compression efficiency. At first, the QNN's typical layers extract visual components such as edges, textures, and patterns. The quantum core of the QNN does supplementary analysis of the collected features. This core utilizes the principles of quantum superposition, quantum gates, and qubits to effectively compress data by simultaneously encoding many versions of the data. The condensed quantum information is deciphered following quantum processing, and the image is reconstructed using conventional image processing methods or inverse operations. Quantum neural networks have the potential to outperform classical approaches due to their ability to process information more effectively through the utilization of superposition and parallelism. QNNs can utilize quantum entanglement as a means to enhance data representations. Moreover, using quantum techniques such as quantum amplitude estimation or Fourier transforms could increase compression ratios and faster processing speeds [4]. This would make QNNs an attractive choice for advanced photo compression.

Quantum neural networks may be able to compress and decompress images effectively using ideas from quantum computing. Image compression aims to minimize file size without compromising visual quality [5]. DCT and quantization are used in JPEG (Joint Photographic Experts Group) compression. Quantum superposition allows QNNs to process and encode multiple states. This could reduce redundancy and increase compression ratios when encoding visual data. Image features can be extracted in quantum parallel by quantum circuits in QNNs. This feature extraction method could produce more compressed, perceptually accurate representations. Compression is optimized using variational quantum circuits and parameterized quantum circuits optimized via classical feedback. These circuits can change parameters to improve compression and reduce reconstruction error. Entanglement is a quantum phenomenon that can enhance the fidelity and compression efficiency of encoding and decoding qubit states. The development of QNN-based image compression systems [44], [45] is challenging due to qubit coherence times and error rates, among other problems with quantum hardware [43]. Quantum computing technology and efficient error correction are required to overcome these limitations. It is challenging to develop training and optimization algorithms for QNN image compression. Mixed classical quantum techniques are needed for QNN training for image compression. All new image compression techniques, including those based on QNNs, must be JPEG-compatible to be valuable and practical. Theoretical and applied research on quantum computing technologies will lead to new quantum-enhanced image compression techniques with higher compression ratios or better visual quality.

A. CONTRIBUTIONS OF THIS PAPER

- We combine quantum entanglement, parallelism and superposition, and quantum algorithm exploration to perform image compression.
- Using a QANN model, image compression could be achieved by extracting features and compressing the feature representation using quantum processing. Inverse operations or classical image processing techniques reconstruct the image from its compressed representation.
- The proposed QANN model improves peak signal-to-noise ratio (PSNR) and structural similarity index

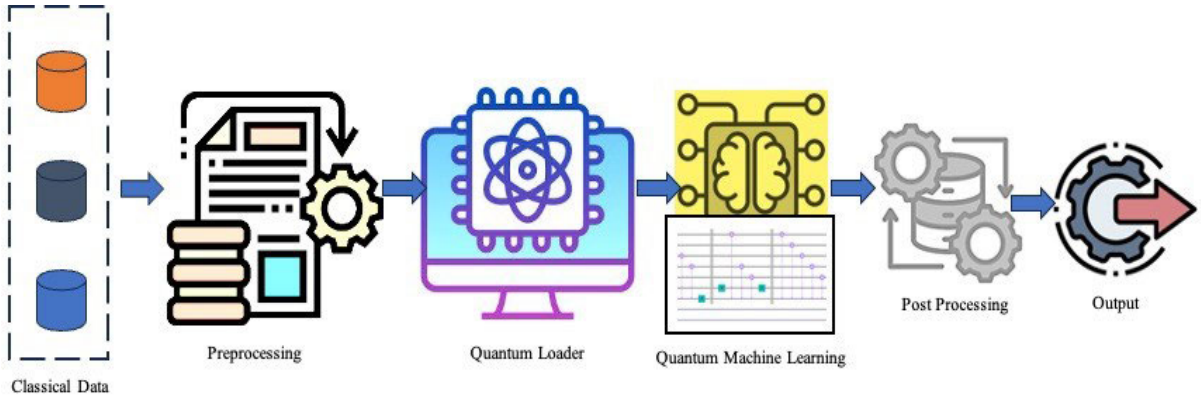

FIGURE 1. Represents steps of quantum machine learning.

(SSIM). It also reduces image size for MRI (73.3%), X-ray (74.1%), and CT-SCAN (71.8%) to save space.

B. ORGANIZATION OF THE PAPER

The subsequent sections of this document are structured in the following manner: Section II presents an extensive examination of the current body of literature on quantum-enhanced machine learning. It focuses on important approaches, advantages, and constraints highlighted in recent research. Section III provides an indepth explanation of the suggested methodology, which encompasses the creation and execution of quantum machine learning models, approaches for preparing the data, and metrics for evaluating the performance of the models. Section IV showcases the empirical discoveries, contrasts the effectiveness of the suggested quantum models with traditional alternatives, and examines the consequences of the outcomes about the difficulties and possibilities mentioned in the literature study. Section V provides a concise overview of the paper's main contributions, highlights the constraints of the current study, and proposes potential avenues for future research in the field of quantum machine learning.

II. LITERATURE REVIEW

A. LITERATURE SURVEY ON MEDICAL IMAGE COMPRESSION TECHNIQUES

Medical image compression reduces the required storage and transmission space for high-resolution medical images while maintaining diagnostic accuracy. Compression algorithms may effectively handle substantial volumes of data from imaging modalities such as CT, MRI, and X-rays by utilizing sophisticated methods such as wavelet transformations, deep learning, and hybrid approaches. Efficient compression facilitates the rapid retrieval of medical photographs and enhances the convenience of telemedicine, archiving, and remote diagnostics, as shown in Table 1.

The authors combined the logistic chaotic map encryption with k-means clustering compression in reference [27]. This was achieved by making the encryption key space larger and the input image smaller. Metrics such as correlation coefficients, Mean Squared Error (MSE), Peak Signal-to-Noise Ratio (PSNR), and Structural Similarity Index (SSIM) are used to assess the efficacy of the proposed method. This study [28] uses the Kodak dataset to particularly investigate both traditional and new methods of image compression with data loss. The main discussion topics are principal component analysis (PCA), K-means, autoencoders, and the Discrete Wavelet Transform (DWT). According to the study, there is a relationship between SSIM and K values, and greater K values imply longer processing times. The research findings

TABLE 1. Examination of methodologies for medical image compression.

Ref	Methodology	Dataset	PSNR (dB)	SSIM
[29]	Compressed sensing algorithm	EEG and DICOM dataset	30.86	0.7489
[30]	High efficiency video coding	DICOM dataset	63.6	0.864
[31]	Fast Fractal compression	ADNI dataset	45.70	-
[32]	Crypto-Steganography	CT scan dataset	22.1125	-
[33]	Wavelet-like transform to an end-to-end compression framework	FAFB Dataset, FIB-25 Dataset, CT-Spleen Dataset, Chaos-CT Dataset, MRI-Heart Dataset, Attention Dataset	89.2	-
[34]	Wavelet difference reduction	Histological microscopy images	42.6987	0.9268
[35]	ROI-based JPEG_OPT method	CT and MRI dataset	88.4	0.9667
[36]	DWT-VQ (Discrete Wavelet Transform – Vector Quantization)	DICOM dataset	71.27	0.8801
[37]	Hybrid adaptive block-based compressive sensing (HABBCS)	NA	38.4877	0.9954
[38]	Energy based Adaptive Block Compressive Sensing (EABCS)	Underwater IoUT images	36.33	0.9543
[39]	Coefficient Mixed Thresholding based ABCS (CMT-ABCS)	DICOM dataset	42.4155	0.985

show that when the value of K is set to 16, the K-means algorithm performs at its best.

Medical signals and images from Digital Imaging and Communications in Medicine (DICOM) and Electroencephalogram (EEG) signals are used as illustrative data for the intended scope of this planned project [29]. A medical facility provides EEG readings obtained using 16 different electrodes. Based on their statistical characteristics, these signals are combined to create a single composite signal, which is then used as input for the CS algorithm. The composite signal is converted into the frequency domain, and the relative power in various frequency ranges is calculated to identify Alzheimer's disease. Increased complexity in storage and operations. In particular, the suggested method allows biological data to be compressed with a ratio as high as 50:1. The proposed method for DICOM image compression yields about 15% improvement in SSIM, 4% improvement in PSNR, and 94% reduction in RT compared to standard CS-based compression.

The high-efficiency video coding (HEVC) application for diagnostically appropriate medical image compression is presented in [30], emphasizing compression efficiency relative to JPEG 2000. This work investigates the use of lossy compression algorithms appropriate for diagnostic purposes and looks at the challenge of compressing high-bit-depth medical images. Using a medically acceptable compression range for JPEG 2000 as a guide, this work establishes a reasonable range of HEVC compression for medical imaging applications. Comparing HEVC to JPEG 2000, experimental results show that the compression efficiency can be increased by over 54%. Concurrently, an innovative technique is suggested to lessen the intricacy of HEVC encoding for medical pictures. According to the findings, HEVC intra-encoding difficulty can be lowered by roughly 55% with only a slight increase in file size.

This study employs fractal-based algorithms to suggest an efficient method for compressing MRI images. The initial step in generating the picture sequence using fractal compression involves converting three-dimensional (3D) MRI scans into a two-dimensional (2D) sequence of images. The inherent spatiotemporal similarity of the 3D objects determines the categorization of range and domain blocks. The suggested strategy enhances the effectiveness of data matching by utilizing self-similarity to decrease the number of blocks in the matching pool. High-quality MRI image decompression is achieved using a residual compensation approach. The test results indicate that the peak signal-to-noise ratio has experienced an almost tenfold rise while the compression speed has improved by two to three. The study demonstrates the effectiveness of the proposed technique in achieving a high compression ratio while maintaining excellent quality in MRI medical pictures [31]. After a thorough discussion of previous work on medical image compression approaches, the topic of quantum-enhanced machine learning, which can be used to address challenges in medical image compression, is discussed.

B. LITERATURE SURVEY ON QUANTUM-ENHANCED ML

This section provides a comprehensive literature overview of multiple works on quantum-enhanced ML. It focuses on the key approaches, benefits, and limits highlighted in recent studies. Our objective is to offer a thorough comprehension of quantum ML's present condition and its capacity to surpass classical techniques despite the obstacles related to scalability and hardware constraints.

Authors [6] aims to assess the viability, precision, and efficiency of a new quantum support vector machine (SVM) formulation for direct multiclass classification using quantum annealing, referred to as quantum multiclass SVM (QMSVM). The authors demonstrate the practical implementation of this strategy utilizing remote sensing data and the latest quantum annealing hardware. The QMSVM developed in this study reflects an accuracy comparable to traditional SVM approaches. The authors in [7] refer to Q-SupCon, an acronym for Quantum-Enhanced Supervised Contrastive Learning Architecture within the Representation Learning Framework. The Q-SupCon model, although performing better than the classical supervised contrastive learning model and hybrid quantum-classical model in situations with limited data, has a slower rate of convergence compared to these models. This implies that although it may get a high level of accuracy, even when there is a lack of data, the duration required to train and fine-tune the model may be significant. Furthermore, the execution of the entire procedure on actual quantum gear was discovered to be excessively costly due to the substantial number of needed iterations. The work [8] aims to tackle the worldwide health issue presented by cardiovascular diseases, which are a prominent contributor to mortality and disability. Given the increasing prevalence of cardiovascular diseases (CVDs), there is a pressing requirement for timely identification and precise categorization of these conditions to enhance treatment results. The study investigates the capacity of Quantum Machine Learning to improve the accuracy of multiclass classification of CVDs compared to traditional machine learning approaches. This is achieved by utilizing the computational benefits of quantum computing, such as the ability to execute numerous parallel computations and overcoming the limitations of classical artificial intelligence methods.

The paper [9] introduces a quantum computing method for categorizing galaxies according to their shape. The study investigates the capacity of quantum computers to enhance the precision of galaxy classifications by using the expansive dimensionality of quantum Hilbert space. The primary objective of the work is to create and utilize a quantum-enhanced SVM algorithm. This approach relies on calculating a kernel matrix, executed on a simulated quantum computer using a quantum circuit that is believed to be challenging to simulate on conventional computers. The results demonstrate that classical and quantum-enhanced SVM algorithms exhibit comparable performance in distinguishing between elliptical and spiral galaxies. With a training size of 40,000 pictures, both techniques yield an area

TABLE 2. Advantages and disadvantages of existing medical image compression methods.

Ref.	Methodology	Pros	Cons
[14]	Proposes a distance-based quantum classifier enhanced with quantum amplitude amplification.	Demonstrates improved classification accuracy on benchmark datasets.	Limited scalability with increasing dimensionality of feature space.
[15]	Utilizes quantum-inspired neural networks for breast cancer classification.	Achieves competitive classification performance compared to classical models.	Requires significant computational resources for training.
[16]	Implements quantum-enhanced support vector machines for large-scale image classification tasks.	Shows improved classification accuracy and reduced training time compared to classical SVMs.	Limited to binary classification tasks.
[17]	Develops a distance-based quantum classifier for machine learning tasks involving categorical variables.	Handles categorical data effectively without the need for one-hot encoding.	Limited experimentation on real-world datasets.
[18]	Proposes a quantum circuit learning framework for image classification tasks.	Demonstrates potential for capturing complex image features using quantum circuits.	Requires further optimization for scalability to large datasets.
[19]	Develops quantum-inspired machine learning algorithms for heart disease classification from medical data.	Shows promising results in early detection of heart disease with improved accuracy.	Limited interpretability of quantum-inspired features.
[20]	Investigates the application of quantum deep learning models for classifying neurological disorders from brain imaging data.	Demonstrates potential for identifying subtle brain abnormalities with high accuracy.	Requires extensive computational resources for training deep quantum networks.
[21]	Proposes a quantum k-nearest neighbor algorithm for classification tasks.	Utilizes quantum superposition and entanglement for efficient classification.	Limited scalability with increasing dataset size and dimensionality.
[22]	Develops quantum-inspired kernel methods for classification using quantum feature maps.	Offers a flexible framework for incorporating quantum features into classical classifiers.	Requires optimization of kernel parameters for different datasets.
[23]	Introduces quantum fuzzy clustering algorithms for multi-class classification tasks.	Handles overlapping clusters and noisy data effectively.	Limited scalability for large datasets due to computational complexity.
[24]	Explores using entangled qubits in quantum machine learning models for document classification.	Shows potential for capturing semantic relationships between documents.	Limited evaluation on real-world text datasets.
[25]	Proposes quantum clustering algorithms for unsupervised classification tasks.	Offers a quantum approach to identifying hidden patterns in data.	Limited to small-scale datasets due to computational constraints.
[26]	Investigates using quantum deep belief networks for sentiment analysis tasks.	Captures complex linguistic features for sentiment classification.	Limited evaluation on large-scale text corpora.

under the receiver operating characteristic curve of 0.946 ± 0.005. Furthermore, the research examines the effectiveness of the quantum SVM algorithm on a quantum computer with noise-mitigation approaches and verifies its consistency with simulation findings. This study represents one of the initial attempts to utilize quantum ML in astronomy, indicating the possibility of employing these techniques in a wider range of applications. The research paper [10] explores the application of quantum computing to enhance anomaly detection in surveillance video data. The objective is to create a hybrid model that combines quantum computing and deep learning approaches, specifically a Convolutional Neural Network (CNN) based on Quantum Computing. The primary objective of this approach is to efficiently extract distinctive characteristics and accurately categorize irregular occurrences, such as traffic accidents and unlawful incidents, from surveillance film. The study presents the actual amplitude circuit based on quantum principles designed to improve performance. The QC-CNN model underwent testing on the UCF-Crime dataset, resulting in an impressive accuracy rate of 95.65 percent, surpassing the performance of previous models. The paper [11] presents a semi-supervised machine learning technique designed for one-class classification that is well-suited for noisy intermediate-scale quantum computing. The variational quantum one-class classifier approach utilizes a fully parameterized quantum autoencoder trained using a conventional dataset and does not necessitate decoding. The research [12] highlights the utilize of the VQOCC (Vector Quantization-based One-Class Classifier) for differentiating standard data from anomalous data. This makes it a valuable tool for detecting anomalies in many domains, such as finance, bioinformatics, and computer vision. The VQOCC is contrasted with conventional machine learning methods, such as the one-class support vector machine, kernel principal component analysis, and deep convolutional autoencoders. Numerical tests were conducted to evaluate performance on datasets such as handwritten digits and Fashion-MNIST. The findings indicate that the classification performance of VQOCC is similar to that of OC-SVM and PCA. However, VQOCC has the advantage of its model parameters increasing only logarithmically with the data size. In addition, the research states that the quantum algorithm consistently performed better than the deep convolutional autoencoder when trained under

comparable settings. This indicates that VQOCC is a very efficient and effective model for OCC.

The paper [13] presents a comprehensive examination of the present condition and future possibilities of quantum computing, with a specific emphasis on the period referred to as NISQ, which stands for Noisy Intermediate-Scale Quantum technology. Preskill elucidates the obstacles and prospects of quantum computing in the NISQ era, examining the constraints arising from error rates and the number of qubits, which serve as the fundamental components of quantum information. The paper highlights that although quantum computers with thousands of qubits will necessitate millions of physical qubits for error correction and are unlikely to be accessible soon, the NISQ technology still offers possibilities to conduct experiments and potentially expedite solutions for intricate problems. The author acknowledges that quantum systems have the potential to surpass conventional computers in replicating complexly interconnected quantum systems. The paper discusses the potential commercial and investment opportunities of quantum computing technology. It suggests that although optimism exists, caution should be exercised due to uncertainties over its short-term applications. In addition, Preskill explores the emerging scientific domain made possible by quantum computing, known as the entanglement frontier. This frontier can potentially drive progress in comprehending intricate molecules, material characteristics, and fundamental principles of physics. The study effectively communicates the enthusiasm within the scientific community for the NISQ era while also promoting a pragmatic outlook on immediate practical uses and highlighting the significance of ongoing endeavors to enhance quantum hardware and algorithm design. Other papers on QC are summarized in Table 2, along with their pros and cons.

This work [32] aims to improve the security of the JPEG compression processor, which is used in medical imaging systems to generate compressed medical images for diagnostic use. The suggested work aims to build a dual defensive mechanism to improve the security of the JPEG compression processor. This technique incorporates hardware steganography and powerful structural obfuscation to defend against recognized threats like Trojan insertion and counterfeiting/cloning. Authors present aiWave [33], an adaptable system that supports lossy and lossless approaches and fully compresses volumetric images. Entropy coding, learning 3-D affine wavelet-like forward and inverse transforms, quantization, and configurable post-processing are all covered by aiWave's components. This technique is significant because it's the first to minimize the size of a picture using an affine wavelet-like transform. You can use this method instead of traditional wavelet transforms because it is more intuitive and adaptable. Additionally, aiWave tests several weight-sharing strategies that are customized based on the details of the data. In doing so, fewer parameters are used without compromising performance.

This study [34] introduces a novel and improved method based on color wavelet difference reduction for compressing medical photos. The proposed method advances the commonly employed wavelet difference reduction (WDR) technique. It utilizes the mean difference between co-located pixels to select the optimal number of color images exhibiting the most significant similarity in time and space. Coherent photos that are large and cover a wide range of time and space are compressed into a single volume and evaluated using the SSIM and PSNR. This method was evaluated using 31 colorectal cancer slides in the challenging domain of histopathology microscope image analysis. The perceptual quality of the medical image is deemed to be exceptionally outstanding. Based on the results, the potential improvement in PSNR compared to JPEG 2000 using existing approaches might reach 22.65 dB. In addition, it can get a maximum improvement of 10.33 decibels compared to a discrete wavelet transform (DWT) technique. Due to these factors, we have introduced a mobile and web platform that enables the compression and transmission of real-time microscopic medical images.

Authors [35] enhanced the performance of JPEGXT (JPEGXT_OPT) and JPEG by utilizing the entire body as the region of interest (ROI) and amplifying the discrete cosine transform coefficients. Our research indicates that ROI figures substantially impact the conversion rate. More precisely, a decrease in return on investment (ROI) within the range of 10-30% leads to an increase in conversion rate (CR). When utilized for near-lossless compression, JPEGXT_OPT can process compression ratios (CRs) of up to 4.0 for regions of interest (ROIs) that occupy 10 to 30% of the image. The compression ratio for more extensive regions of interest (ROIs) that cover 90-100% of the image is just 1.2. The compression ratios achieved using JPEG_OPT are significantly higher. By maintaining a low ROI (Return on Investment) ranging from 10% to 30%, it is possible to compress CT (Computed Tomography) and MRI (Magnetic Resonance Imaging) images above a threshold of 20.0.

This research suggests compressing images using DWT-VQ (Discrete Wavelet Transform – Vector Quantization) while retaining medically acceptable visual quality. This hybrid strategy lowers ultrasonic speckle and salt and pepper noises. The procedure has little effect without ultrasound, but the edge is intact. The visualsThe data is then filtered using a DWT. When dealing with intricate medical imaging, it is recommended to use Vector Quantization (VQ) to preserve diagnostic information. To differentiate between the two main strategies, it is recommended to use an intermediate approach that produces wavelet coefficients. To increase the probability of consecutive zeros, the quantizer functions optimally by setting any integer below the threshold to zero. To achieve the appropriate dimensions, a codebook is augmented with a codeword comprised entirely of zeros at its inception. Thresholding has minimal impact on the restored image. The Huffman algorithms encode the coefficients following the completion of the final codebook. The most effective hybrid method is achieved by employing two stages of DWT before quantization [36]. This work [37]

introduces Hybrid adaptive block-based compressive sensing (HABBCS), a very efficient hybrid technique. HABBCS calculates the mean value of the frame by first determining the sampling rate of each block inside a frame using an adaptive estimate. Consequently, these typical frames are utilized to calculate the overall sampling rate of the film, and BBCS is employed to compress the video. Performance indicators such as PSNR, Delta E, Video Structural Similarity Index (VSSIM), and Computational Time (CT) are calculated and displayed. Based on the findings, HABBCS performs better than ABBCS, with faster data processing capabilities.

This work presents an Orthogonal Matching Pursuit reconstruction approach coupled with Energy-based Adaptive Block Compressive Sensing (EABCS) [38] to enhance the reconstructed image's visual quality and sampling performance. Because it is extremely sparse, the sparse binary random matrix is employed as the measurement matrix. Under this energy-based adaptive technique, blocks with more energy are allocated higher measurements, and blocks with lower energy are assigned lower measures. When it comes to measurements and samples, the suggested EABCS technique performs better than current adaptive techniques in terms of compression, with a rate of about 25–30%. It also causes a structural similarity index of roughly 0.1-0.3 and an increase in the Peak signal-to-noise ratio of about 3-5 dB. Approximately 60–70% of the area is kept open. This paper presents the CMT-ABCS approach [39], which compresses different medical images at a high compression ratio using Coefficient Mixed Thresholding. The experimental results show a notable improvement in the performance measures of the proposed strategy over the state-of-the-art approaches. The Structural Similarity Index (SSIM) has improved by 0.1–0.2, the Peak Signal-to-Noise Ratio (PSNR) by 5–10 dB, and the Normalized Cross-Correlation (NCC) and Normalized Absolute Error (NAE) by 0.1–0.2. With only around 10% of the measurements or samples, the reconstruction was much enhanced at a moderate sampling rate.

Because of its ability to handle complicated, high-dimensional data, quantum machine learning has the potential to transform medical image processing and compression completely. Through sophisticated feature extraction, segmentation, and classification, quantum approaches can improve the diagnostic accuracy of medical imaging, including MRI, CT, and ultrasound. This will benefit applications such as tumor detection and the diagnosis of cardiovascular disease. In addition, by detecting and preserving diagnostically important information more effectively than classical techniques, quantum algorithms can optimize image compression, allowing faster storage and exchange of medical data without compromising quality. However, barriers such as slower convergence rates, high computational costs, and technology limitations make practical implementation difficult. By overcoming these barriers through advances in quantum hardware and algorithm design, scalable and effective solutions could be made available, revolutionizing telemedicine, treatment planning, and medical diagnostics.

III. PROPOSED QANN MODEL

Medical image compression is essential because imaging modalities such as MRI, CT, and X-rays generate enormous amounts of data that can strain storage systems, limit data transfer, and hinder real-time processing. Effective compression reduces costs and increases accessibility by ensuring these images can be transmitted and stored without compromising diagnostic quality. These requirements are met by Quantum-Enhanced Artificial Neural Networks (QANN), which use quantum computing to process high-dimensional, complicated medical data more efficiently than traditional techniques. QANNs are ideal for telemedicine, remote diagnostics and real-time healthcare decision-making applications because they retain diagnostically important properties while achieving better compression ratios and faster processing times. By improving scalability, this cutting-edge method helps healthcare systems meet increasing data demands while maintaining effectiveness and quality.

Quantum-Enhanced Artificial Neural Networks (QANN) are used in medical image compression. Using quantum concepts such as superposition, QANN effectively extracts features and eliminates redundancy, preserving diagnostic quality while achieving high compression ratios. This enables faster transmission and storage, particularly for bandwidth-dependent applications such as telemedicine. The process is further accelerated by quantum parallelism, making it ideal for real-time applications. However, hardware limitations and system noise must be addressed to ensure scalability and clinical reliability. QANN could completely transform medical imaging, improving healthcare and diagnosis.

Here, our concept combines quantum computing with traditional machine learning approaches to improve the performance of multiclass classification. Firstly, the incoming data is subjected to classical preprocessing, which involves standardization to prepare it for quantum state encoding. Next, the standardized data is converted into quantum states via unitary operations, allowing for processing in the quantum realm. The Quantum-Enhanced Artificial Neural Network is an innovative method combining the principles of quantum computing with classical neural network structures to enhance the performance of supervised learning tasks. The purpose of this hybrid model is to use the computing benefits of quantum mechanics, specifically in managing extensive and intricate datasets that present substantial difficulties for conventional machine-learning methods.

Given a dataset $\mathcal{D} = \{(x_i, y_i)\}_{i=1}^{N}$ where $x_i \in \mathbb{R}^d$ are the feature vectors and $y_i \in \{1, \ldots, c\}$ are the class labels.

$$z_i = \frac{x_i - \mu}{\sigma} \tag{1}$$

where μ is the mean and σ is the standard deviation of the dataset features.

$$|\psi_i\rangle = U(Z_i) \vee |0\rangle \tag{2}$$

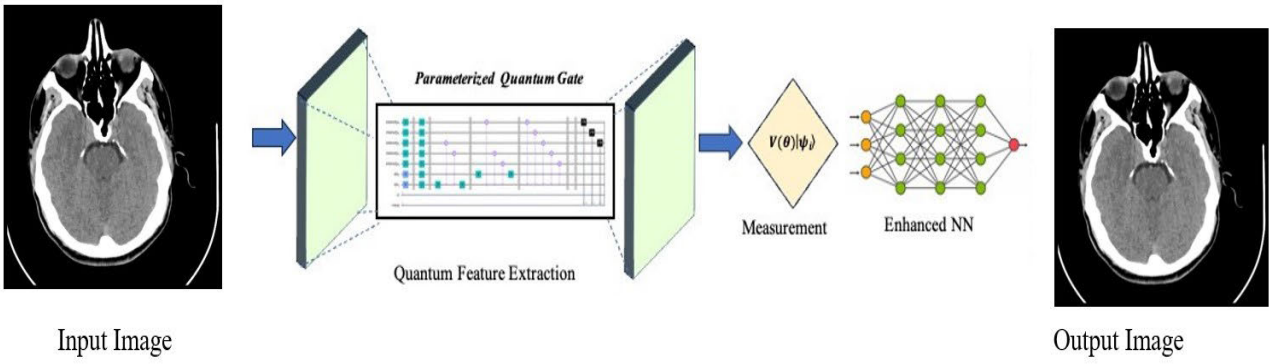

FIGURE 2. Proposed QANN model.

where $U(z_i)$ is a unitary transformation that encodes the classical data z_i in the quantum state $|\psi_i\rangle$.

$$|\varphi_i\rangle = V(\theta)\,|\psi_i\rangle \tag{3}$$

$V(\theta)$ defines a parameterized quantum circuit with parameter θ.

$$q_i = \text{Measurement}(|\varphi_i\rangle) \tag{4}$$

Let q_i be the quantum extracted features. A classical neural network is defined with weights W_l and activation function f.

$$h_0 = q_i \tag{5}$$

h_0: Input layer
For each layer $l = 1, 2, \ldots, L$

$$h_l = f(W_l h_{l-1} + b_l) \tag{6}$$

where W_l and b_l are the weight matrix and bias vector for layer l.

$$(\hat{y}_i)^l = f(W_l h_{l-1} + b_l) \tag{7}$$

We use cross-entropy loss for classification

$$L(w, \theta) = -\frac{1}{N}\sum_{i=1}^{N}\sum_{c=1}^{C} 1\{y_i = c\}\log((\hat{y}_i), c) \tag{8}$$

where $1\{y_i = c\}$ is an indicator function that is 1 if $y_i = c$ and 0 otherwise.

Optimize the parameters W and θ using gradient-based methods such as stochastic gradient descent.

$$(\hat{w}, \hat{\theta}) = \arg\min L(w, \theta) \tag{9}$$

Quantum data augmentation is applied to quantum circuit

$$q_i^{\text{aug}} = V_{\text{aug}}(q_i) \tag{10}$$

where V_{aug} is a parameterized quantum circuit for augmentation.

A. QANN IMAGE COMPRESSION

Data preprocessing is essential to improve model performance, especially for tasks such as medical image classification. The architecture of Quantum-Enhanced Multiclass Classification used in medical imaging is shown in Fig 2. This section presents a novel approach to medical image data preparation, which involves converting images to greyscale and scaling them to dimensions that have a power of 2. While greyscale conversion facilitates data representation without sacrificing diagnostically significant features, scaling to a power of two increases computational efficiency and optimizes memory usage. Several models and medical imaging datasets are used to evaluate the processing technique, which shows that it improves model performance. The reduced computational load makes this method suitable for large-scale medical applications, including telemedicine and disease diagnosis. The preprocessing methods lay the foundation for more effective and accurate machine-learning models in medical imaging.

Our proposed preprocessing strategy involves resizing input to dimensions that are exponential multiples of 2, such as 32×32, 64×64, 128×128, and so on. The selection of this resizing technique is based on maximizing memory consumption and computational efficiency, particularly in GPU-accelerated computing environments where power-of-2 dimensions are more effective for processing. To preserve the quality of the data during the resizing process, interpolation techniques are used. These techniques allow for alterations in size while retaining critical visual details. The objective of adopting this resizing method is to optimize the preprocessing pipeline by ensuring the integrity of the image data for subsequent machine-learning activities.

Resizing data to a power of 2 means altering their dimensions to be a multiple of 2, which is a typical requirement for many compression methods, including those based on quantum technology. Resizing an image usually requires interpolation to preserve its quality. Bilinear interpolation is a frequently used method for interpolation. It calculates the new pixel values by blending the values of nearby pixels.

Let's consider an example: Suppose we have an image with dimensions 600×400 pixels. To resize it to the nearest

power of 2, we would resize it to 512 × 512 pixels. 3. As part of the preprocessing workflow, RGB photos are transformed into grayscale by calculating weighted averages of their red, green, and blue channels. This conversion streamlines the data representation by merging color information into a solitary channel, decreasing input dimensions and computational complexity. Grayscale conversion improves the ability to extract features by emphasizing brightness and ignoring color differences. This allows machine learning models to better concentrate on important medical image attributes for categorization.

Algorithm 1 Preprocessing for Data Classification

Input: Original dataset

Step 1 For each data sample in the dataset: If image- Read the image and extract its dimensions (width and height).

Step 2 For each image in the dataset:

Resize the image to the nearest power of 2:

Calculate the next power of 2 for both width and height:

$\textbf{new\_width} = 2^{\lceil \log_2(\text{original\_width}) \rceil}$

$\textbf{new\_height} = 2^{\lceil \log_2(\text{original\_height}) \rceil}$

Resize the image using bilinear interpolation to **new_width** × **new_height** dimensions.

Step 3 For each resized image in the dataset:

Convert the RGB image to grayscale: For each pixel (x, y) in the image

Extract the RGB values (R, G, B) of the pixel.

Compute the grayscale intensity (I) using the formula:

$I = 0.2989 \cdot R + 0.5870 \cdot G + 0.1140 \cdot B$

Set the pixel value at (x, y) to the computed grayscale intensity (I).

Output The compressed grayscale images.

According to Algorithm 1, if the data is a medical image, the Image preprocessing for compression algorithm seeks to convert original RGB images into preprocessed grayscale images to prepare them for compression. At first, the algorithm retrieves each medical image from the collection and obtains its dimensions, such as width and height. Afterward, it resists each image to the closest power of 2. This requires performing logarithmic operations to get the next power of 2 for both the width and height to optimize memory usage. Subsequently, the medical image is proportionally adjusted to the computed dimensions with bilinear interpolation, so maintaining the integrity of the image throughout the resizing procedure. During the subsequent stage, the algorithm transforms the RGB representation of each scaled image into grayscale. The conversion process involves iterating through each pixel in the medical image, extracting the RGB values, and calculating the grayscale intensity by applying a weighted sum of the RGB components. Ultimately, the algorithm produces preprocessed grayscale images, which have been enhanced for compression. This is achieved by consolidating the color information into a single channel, making storing and transmitting the images easier. In summary, the preprocessing pipelines guarantee that the medical images are correctly downsized and transformed to grayscale, allowing for efficient compression techniques. This ultimately leads to a reduction in storage needs and transmission bandwidth while still maintaining crucial visual information. Bilinear interpolation is a widely employed method for approximating values within a grid created by four adjacent pixels. The operation involves calculating a weighted average of these pixels to estimate the value of a point between them. Bilinear interpolation is a mathematical method used to determine the interpolated value (I) based on four-pixel values (p_{00}, p_{01}, p_{10}, and p_{11}) and their relative distances to the target point (x, y).

$$I = (1-\alpha)(1-\beta)p_{00} + \alpha(1-\beta)p_{10} + (1-\alpha)\beta p_{01} + \alpha\beta p_{11} \tag{11}$$

The symbols α and β denote the proportional distances between the target point and the adjacent pixels along the horizontal and vertical axes. This technique efficiently combines the adjoining pixel values to create a seamless transition between them, which is invaluable for scaling photos and other types of spatial data interpolation.

B. RGB TO GRAY SCALE

The grayscale intensity for each pixel is determined by combining the RGB values using weights based on each color channel's perceived luminance to convert RGB photos to grayscale. Mathematically, the grayscale intensity (I) of an RGB pixel represented as (R, G, B) is determined using the following formula:

$$I = 0.2989R + 0.5870G + 0.1140B$$

The coefficients 0.2989, 0.5870, and 0.1140 in (12) represent the weights allocated to the red, green, and blue channels, respectively. The weights are designed to align with the human visual system's sensitivity to various colors. They aim to generate a grayscale depiction that retains crucial visual details while eliminating color discrepancies. By utilizing these weighted averages, the conversion procedure efficiently streamlines the data representation, decreasing input dimensions and computing complexity while preserving the essential elements required for subsequent analysis and processing.

Quantum data augmentation enhances the dataset by introducing more unpredictability, improving the neural network model's ability to generalize to new and unseen data. By utilizing quantum circuits for augmentation, we exploit the distinctive characteristics of quantum mechanics to generate a wide range of intricate changes that are computationally efficient. The efficacy of the enhanced quantum characteristics is assessed by comparing the performance metrics of the model trained with and without data augmentation. Incorporating quantum data augmentation into the traditional neural network framework enhances the model's performance on regular datasets and creates new opportunities for utilizing quantum computing in machine

learning. This technique shows considerable promise in improving data-driven solutions, especially in fields that handle extensive and intricate information.

C. COMPUTATIONAL COMPLEXITY OF CLASSICAL VS QANN MODEL

This paper categorized the complexity of classical preprocessing complexity and quantum complexity of proposed methods shown in Table 3.

- **Classical preprocessing complexity:**
  In this, each feature is standardized using equation (1), and the complexity of the standardization is $O(n.d)$, where n represents data samples and d represents a number of features. Considering algorithm 1, the next power of 2 for height and width should be calculated, wherein each image is resized using a bilinear equation (11). The complexity of both power of 2 and resizing is $O(n.w.h)$ where n is the number of images, w and h are image dimensions. Similarly, the same complexity is obtained in the grayscale conversion.
- **Quantum processing complexity:**
  Standardized data Z_i is encoded into quantum states using a unitary operation $U(Z_i)$ as follows:

$$|\phi\rangle = U(Z_i)|0\rangle$$

  The complexity of the above standardization data is $O(n.poly(d))$ where d represents the number of qubits. Similarly, the quantum measurements are considered for complexity calculation. It provides O(n.q) where q represents the number of qubits.

TABLE 3. Complexity comparison between classical and QANN.

Taken Component	Classical Complexity	QANN Complexity
Preprocessing	$O(n.d)$	$O(n.(d+w.h))$
Feature Encoding	$O(1)$	$O(n.\text{poly}(d))$
Overall Computational Complexity	$O(n \times L \times k^2)$ where L is the number of layers, k represents average neurons	$O(n \cdot (\text{poly}(d) + g \cdot q + L \cdot k^2))$ where g represents number of gates and q represents number of qubits

IV. RESULT AND DISCUSSION

This section compares our proposed QANN mode with other image compression methods to determine its effectiveness. The results of the studies demonstrated how quantum computing can be used to improve the accuracy and efficiency of medical image compression. We ensured the validity and practicality of our findings by using real-world scenarios in the COVID-CXNet [42] chest x-ray images and the Kaggle brain CT and MRI datasets [41] for our comparison study.

With separate datasets for CT, MRI, and X-ray imaging modalities, the Kaggle dataset "darren2020/ct-to-mri-cgan" provides a comprehensive resource for training and testing medical imaging models. There are 1,742 training images and 744 test images in the CT dataset and 1,744 training images and 744 test images in the MRI dataset. The dataset also includes X-rays, of which 452 are used for testing and 900 for training. Applications such as image synthesis, classification, and diagnosis using sophisticated processing and quantum machine learning techniques are enabled by this balanced distribution across modalities, which facilitates robust model training and evaluation.

The investigations used Python programming and libraries such as scikit-learn for traditional machine learning methods and Qiskit for quantum computing capabilities. To ensure a fair distribution of samples across different classes, we divided the dataset into separate training and testing sets. We will use a comprehensive set of performance metrics to evaluate the effectiveness of the proposed quantum-enhanced classification methods. Several performance measures, such as enhanced peak signal-to-noise ratio (PSNR) and structural similarity index (SSIM), will be evaluated using these metrics. To save space, the image size is reduced for MRI (73.3%), X-ray (74.1%), and CT-SCAN (71.8%) using quantum technology.

A. PEAK SIGNAL-TO-NOISE RATIO (PSNR)

PSNR is a frequently used metric to evaluate how faithfully compressed or reconstructed medical images compare to their sources. PSNR measures the maximum difference between the original and compressed medical image quality; higher PSNR values correspond to higher-quality images.

Compute the PSNR in decibels (dB):

$$\text{PSNR} = 10\log_{10}\left(\frac{L^2}{\text{MSE}}\right) \tag{12}$$

where:

- L is the maximum possible pixel value of the image.
- MSE is the Mean Squared Error.

$$\text{MSE} = \frac{1}{MN}\sum_{i=1}^{M}\sum_{j=1}^{N}[I(i,j) - K(i,j)]^2 \tag{13}$$

where:

- $I(i,j)$ is the pixel value at position (i,j) in the original image.
- $K(i,j)$ is the pixel value at position (i,j) in the compressed image.
- M and N are the dimensions of the images.

PSNR measures how closely the compressed version resembles the original content in Table 4. Higher PSNR values, which indicate lower noise and distortion levels than the original signal, indicate a higher quality reconstruction. The Δ PSNR suggests the difference between the current approaches and our proposed QANN model.

For CT scan images, the PSNR values obtained by E-ABCS, CMT-ABCS, WDR, and DCAE are 27.57, 36.82, 26.43, and 37.05. In contrast, the proposed QANN model achieves a PSNR value of 40.03 compared to all other existing

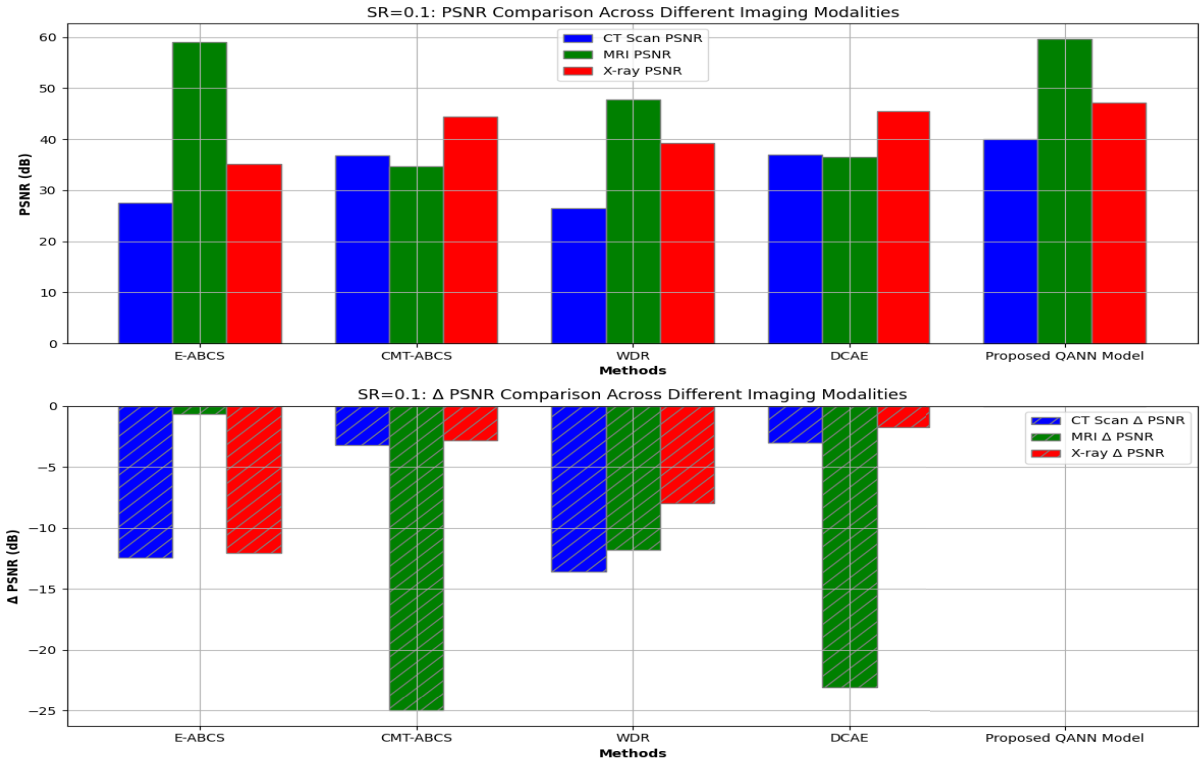

FIGURE 3. Analysis of PSNR and Delta PSNR in SR = 0.1.

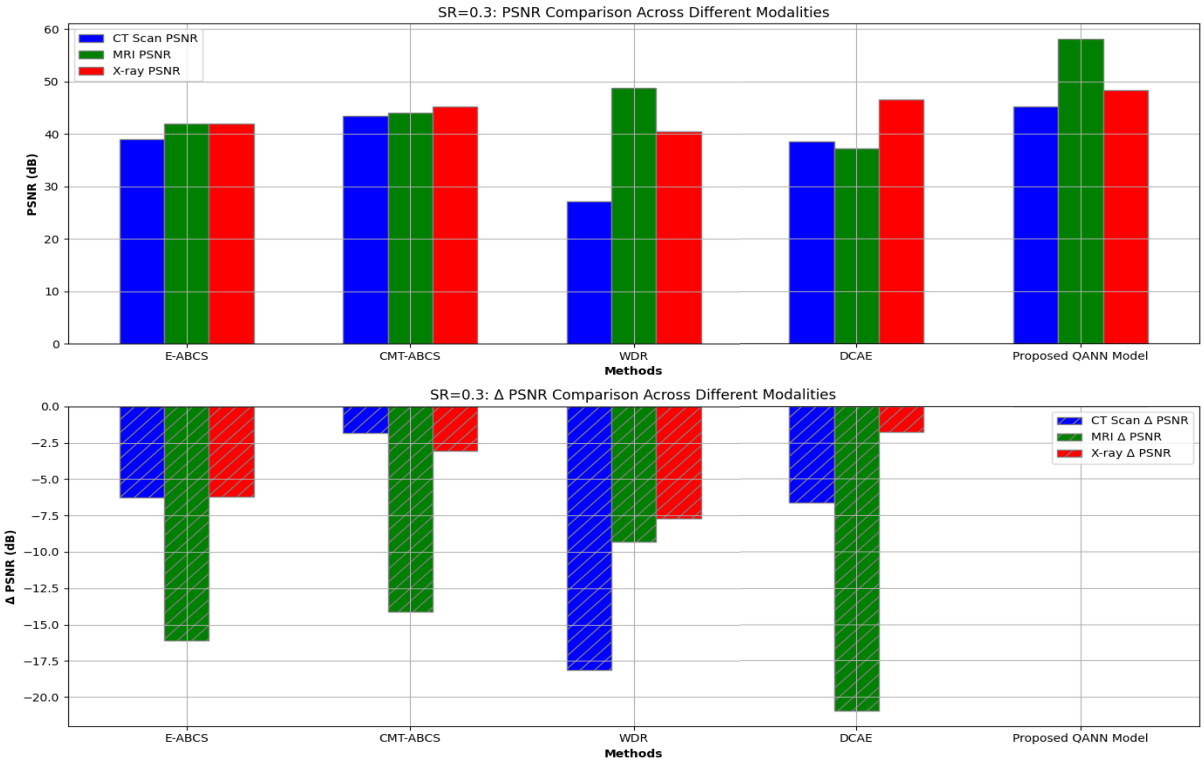

FIGURE 4. Analysis of PSNR and Delta PSNR in SR = 0.3.

approaches with SR = 0.1, as shown in Fig 3. There is less difference in Δ when comparing CMT-ABCS and DCAE with the other current methods. For MRI scans, the PSNR values obtained by E-ABCS, CMT-ABCS, WDR, and DCAE are, in order, 59.01, 34.64, 47.81, and 36.59. Compared to all other current techniques with SR = 0.1, the proposed QANN

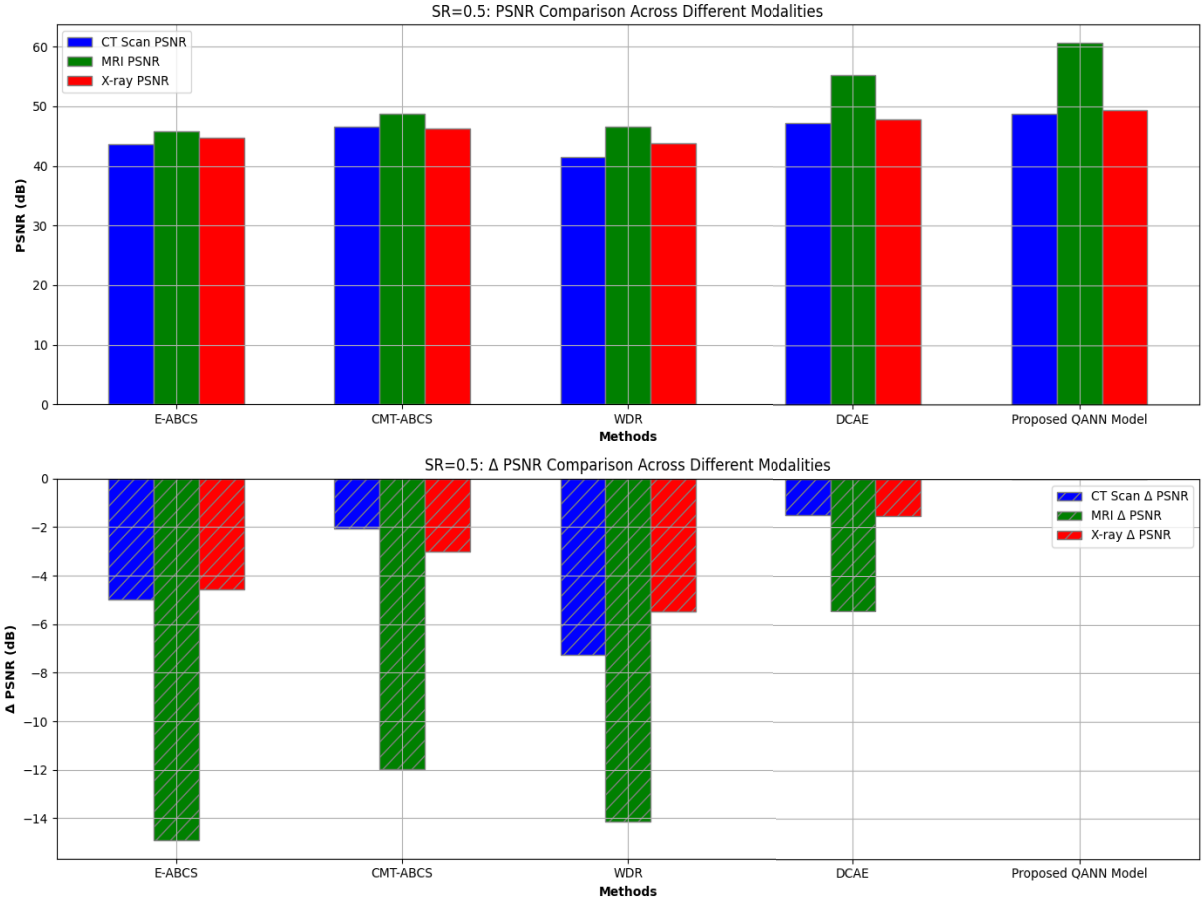

FIGURE 5. Analysis of PSNR and Delta PSNR in SR = 0.5.

TABLE 4. PSNR and Δ PSNR analysis.

Methods	CT scan		MRI		X-ray	
SR=0.1	PSNR	Δ PSNR	PSNR	Δ PSNR	PSNR	Δ PSNR
E-ABCS [38]	27.57	-12.46	59.01	-0.63	35.19	-12.03
CMT-ABCS [39]	36.82	-3.21	34.64	-25	44.38	-2.84
WDR [34]	26.43	-13.6	47.81	-11.83	39.24	-7.98
DCAE [40]	37.05	-2.98	36.59	-23.05	45.47	-1.75
Proposed QANN Model	40.03	NA	59.64	NA	47.22	NA
SR=0.3	PSNR	Δ PSNR	PSNR	Δ PSNR	PSNR	Δ PSNR
E-ABCS WDR [38]	38.95	-2.28	42.02	-16.11	42.04	-6.23
CMT-ABCS [39]	43.41	-2.02	43.99	-14.14	45.2	-3.07
WDR WDR [34]	27.1	-14.13	48.82	-9.31	40.55	-7.72
DCAE [40]	38.61	-2.62	37.17	-20.96	46.49	-1.78
Proposed QANN Model	45.23	NA	58.13	NA	48.27	NA
SR=0.5	PSNR	Δ PSNR	PSNR	Δ PSNR	PSNR	Δ PSNR
E-ABCS [38]	43.67	-5	45.76	-14.9	44.72	-4.57
CMT-ABCS DCAE [39]	46.61	-2.06	48.69	-11.97	46.27	-3.02
WDR [34]	41.4	-7.27	46.52	-14.14	43.8	-5.49
DCAE DCAE [40]	47.2	-1.47	55.21	-5.45	47.76	-1.53
Proposed QANN Model	48.67	NA	60.66	NA	49.29	NA

model achieves a PSNR of 59.64. When comparing E-ABCS with the other existing approaches, there is less difference in the Δ value. E-ABCS, CMT-ABCS, WDR, and DCAE gave PSNR values for X-rays of 35.19, 44.38, 39.24, and 45.47, respectively. Compared to all other known techniques with SR = 0.1, the proposed QANN model achieves a PSNR of 47.22. When comparing CMT-ABCS and DCAE with the other existing approaches, there is less difference in the Δ value.

For CT images, the PSNR values obtained by E-ABCS, CMT-ABCS, WDR, and DCAE are 43.67, 46.61, 41.4, and 47.2, respectively, shown in Fig 4. On the other hand, the

proposed QANN model achieves a PSNR of 48.67 compared to all other methods currently in use with SR = 0.5. When comparing DCAE with the other existing approaches, there is less difference in Δ. The PSNR values for MRI scans obtained by WDR, DCAE, E-ABCS, and CMT-ABCS are 45.76, 48.69, 46.52, and 55.21 in that order. The proposed QANN model achieves a PSNR of 60.66 compared to all other existing methods with SR = 0.5. The difference in Δ value is minor when DCAE is compared with the other current methods. For X-rays, the PSNR values of E-ABCS, CMT-ABCS, WDR, and DCAE were 44.72, 46.27, 43.8, and 47.76, respectively. The proposed QANN model achieves a PSNR of 49.29, higher than any other known approach with SR = 0.5 shown in Fig 5. The Δ value differs less between DCAE and the other current methods. Our proposed QANN model outperforms the existing system in all scenarios compared to SR = 0.5 and SR = 0.1. Furthermore, for SR = 0.1, the CMT-ABCS and DCAE perform very close to our proposed model for CT and X-ray images. In contrast, E-ABCS performs very close to our proposed model for MRI images, DCAE performs very close to our proposed method for CT, MRI and X-ray images el when SR = 0.5.

Table 4 shows that the proposed QANN model produces higher PSNR values than alternative methods at SR = 0.1, with a difference of 1.75 dB-13 dB. A difference of 1.53 dB-15 dB in PSNR is achieved at higher sampling rates. Later in this study, the subjective results show that although some algorithms occasionally produce PSNR values closer to the proposed one, they have poor reconstruction of some blocks. The perceptual metric SSIM is used to quantify how much the reconstructed medical image has changed from the original.

B. STRUCTURAL RESEMBLANCE INDEX (SSIM)

A perceptual metric called the Structural Resemblance Index measures the similarity of two images. Because SSIM considers changes in brightness, contrast, and structural information, it is more in line with how humans see visual stimuli than PSNR, which only analyzes differences in individual pixels. Table 5 shows SSIM comparisons for various medical images.

The SSIM index is calculated using the following formula:

$$\text{SSIM}(x, y) = \left(\frac{2\mu_x\mu_y + C_1}{\mu_x^2 + \mu_y^2 + C_1}\right) \cdot \left(\frac{2\sigma_x\sigma_y + C_2}{\sigma_x^2 + \sigma_y^2 + C_2}\right) \cdot \left(\frac{\sigma_{xy} + C_3}{\sigma_x\sigma_y + C_3}\right) \tag{14}$$

where:

- x and y are the two images being compared.
- μ_x and μ_y are the mean intensity of x and y, respectively.
- σ_x and σ_y are the standard deviations of x and y, respectively.
- σ_{xy} is the covariance of x and y.
- $C_1 = (K_1 \cdot L)^2$
- $C_2 = (K_2 \cdot L)^2$
- $C_3 = C_1/2$
- L is the dynamic range of the pixel values.
- K_1 and K_2 are constants.

The SSIM values for CT images obtained using E-ABCS, CMT-ABCS, WDR, and DCAE are, in order, 0.634, 0.911, 0.657, and 0.928 shown in Fig 6. However, when the proposed QANN model is compared with all other methods currently used with SR = 0.1, the SSIM value is 0.941. When DCAE is compared with the other existing approaches, there is less difference in Δ. The results of E-ABCS, CMT-ABCS, WDR, and DCAE for MRI scans are, in order, 0.716, 0.965, 0.699, and 0.924 for SSIM values. With SR = 0.1, the proposed QANN model gives an SSIM of 0.955 compared to all other existing methods. The difference in the Δ value between DCAE and the other currently used methods is minimal. SSIM values for X-rays were obtained from E-ABCS, CMT-ABCS, WDR, and DCAE in the following order: 0.719, 0.965, 0.8, and 0.976. The proposed QANN model obtains an SSIM of 0.987 compared to all other known methods with SR = 0.1. There is less difference in the Δ value between DCAE and the other current methods.

For CT images acquired with E-ABCS, CMT-ABCS, WDR, and DCAE, the SSIM values are 0.949, 0.968, 0.935, and 0.97, respectively, shown in Fig 7. On the other hand, the SSIM value is 0.989 when the proposed QANN model is compared with all other existing approaches with SR = 0.5 shown in Fig 8. There is less difference in Δ between DCAE and the other current methods. In that order, the E-ABCS, CMT-ABCS, WDR, and DCAE results for MRI scans are 0.969, 0.984, 0.962, and 0.989 for SSIM values. Compared to all other current techniques, the proposed QANN model gives an SSIM of 0.994 with SR = 0.5. There is little difference in the Δ values between DCAE and the other currently used approaches. The following order of SSIM values for X-rays was derived using E-ABCS, CMT-ABCS, WDR, and DCAE: 0.98, 0.985, 0.973 and 0.991. Compared to all other existing techniques with SR = 0.5, the proposed QANN model achieves an SSIM of 0.996. The Δ value differs less between DCAE and the other currently used approaches.

When comparing our proposed QANN model with SR = 0.5, 0.3, and 0.1, we see that it performs better than the current system in every case. It is also shown that the DCAE performs exceptionally well for CT, MRI, and X-ray images for SR = 0.5, 0.3, and SR = 0.1. It is also noted that the SSIM value for SR = 0.5 is much closer to 1 than for SR = 0.3 and SR = 0.1. SSIM values closer to 1 are produced by a good reconstruction algorithm. Table 5 shows that the proposed QANN model outperforms the others in terms of SSIM values. The SSIM values are closer to 1 even at SR = 0.1, while other approaches have lower values. This shows little degradation in the quality of the reconstructed images compared to the original images.

C. IMAGE SIZE AND SPACE ANALYSIS

The sample compression of exiting methods images are shown in Fig 9. Table 6 shows the compressed image size

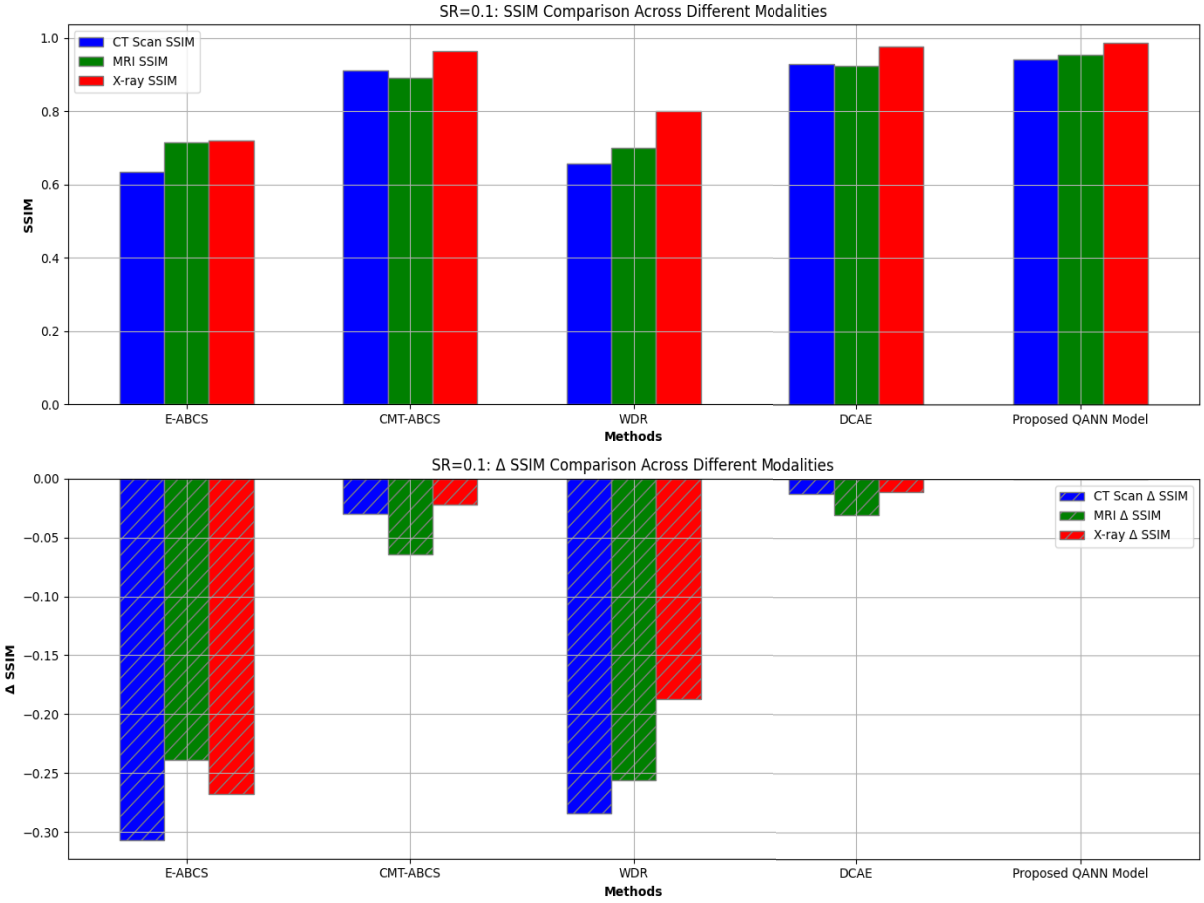

FIGURE 6. Analysis of SSIM and Delta SSIM in SR=0.1.

TABLE 5. SSIM and Δ SSIM analysis.

Methods	CT scan		MRI		X-ray	
SR=0.1	SSIM	Δ SSIM	SSIM	Δ SSIM	SSIM	Δ SSIM
E-ABCS	0.634	-0.307	0.716	-0.239	0.719	-0.268
CMT-ABCS	0.911	-0.03	0.891	-0.064	0.965	-0.022
WDR	0.657	-0.284	0.699	-0.256	0.8	-0.187
DCAE	0.928	-0.013	0.924	-0.031	0.976	-0.011
Proposed QANN Model	0.941	NA	0.955	NA	0.987	NA
SR=0.3	SSIM	Δ SSIM	SSIM	Δ SSIM	SSIM	Δ SSIM
E-ABCS	0.868	-0.106	0.966	-0.02	0.978	-0.015
CMT-ABCS	0.953	-0.021	0.972	-0.014	0.98	-0.013
WDR	0.932	-0.042	0.819	-0.167	0.916	-0.077
DCAE	0.961	-0.013	0.979	-0.007	0.986	-0.007
Proposed QANN Model	0.974	NA	0.986	NA	0.993	NA
SR=0.5	SSIM	Δ SSIM	SSIM	Δ SSIM	SSIM	Δ SSIM
E-ABCS	0.949	-0.04	0.969	-0.025	0.98	-0.016
CMT-ABCS	0.968	-0.021	0.984	-0.01	0.985	-0.011
WDR	0.935	-0.054	0.962	-0.032	0.973	-0.023
DCAE	0.97	-0.019	0.989	-0.005	0.991	-0.005
Proposed QANN Model	0.989	NA	0.994	NA	0.996	NA

and space savings of the CT image for different sampling rates. It also shows that the proposed QANN model achieves high compression levels. As a result, the space-saving values have increased. Furthermore, the proposed solution requires less time to execute the algorithm compared to alternative methods. The space savings for SR = 0.1, 0.3, and 0.5 are 71.8%, 64.4%, and 61.9%, respectively, shown in Fig 10.

Table 7 illustrates the reduced size and space saving of the MRI image for different sampling rates. It also shows that the proposed QANN model has achieved significant compression. For SR = 0.1, 0.3, and 0.5, the space savings

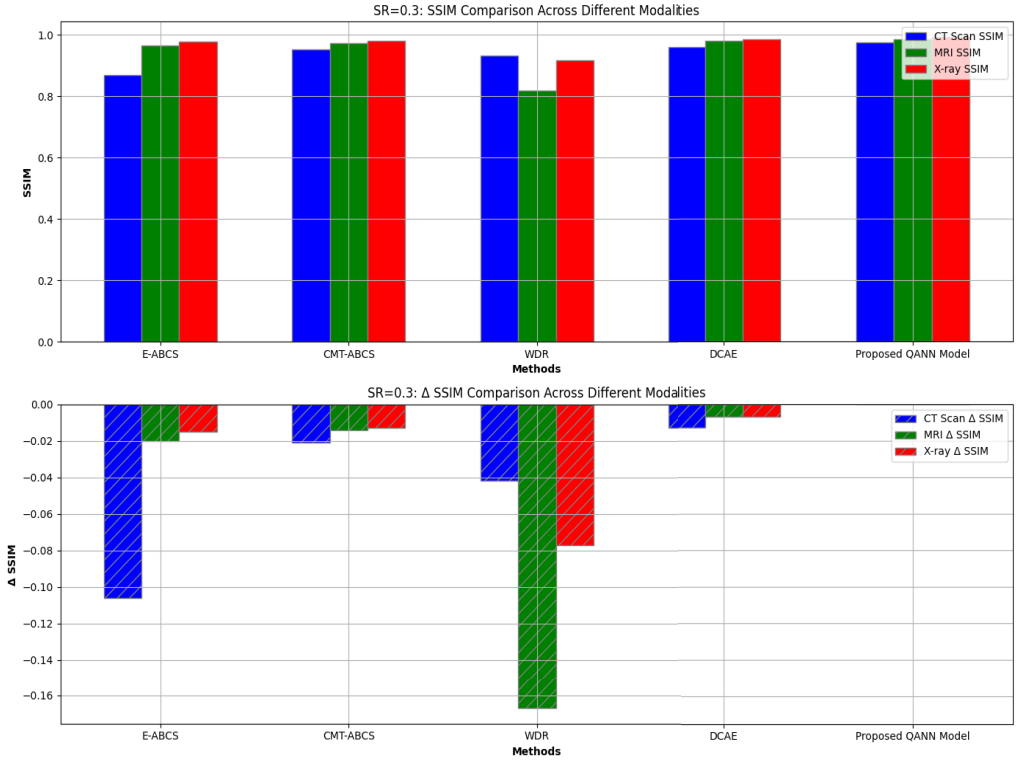

FIGURE 7. Analysis of SSIM and Delta SSIM in SR = 0.3.

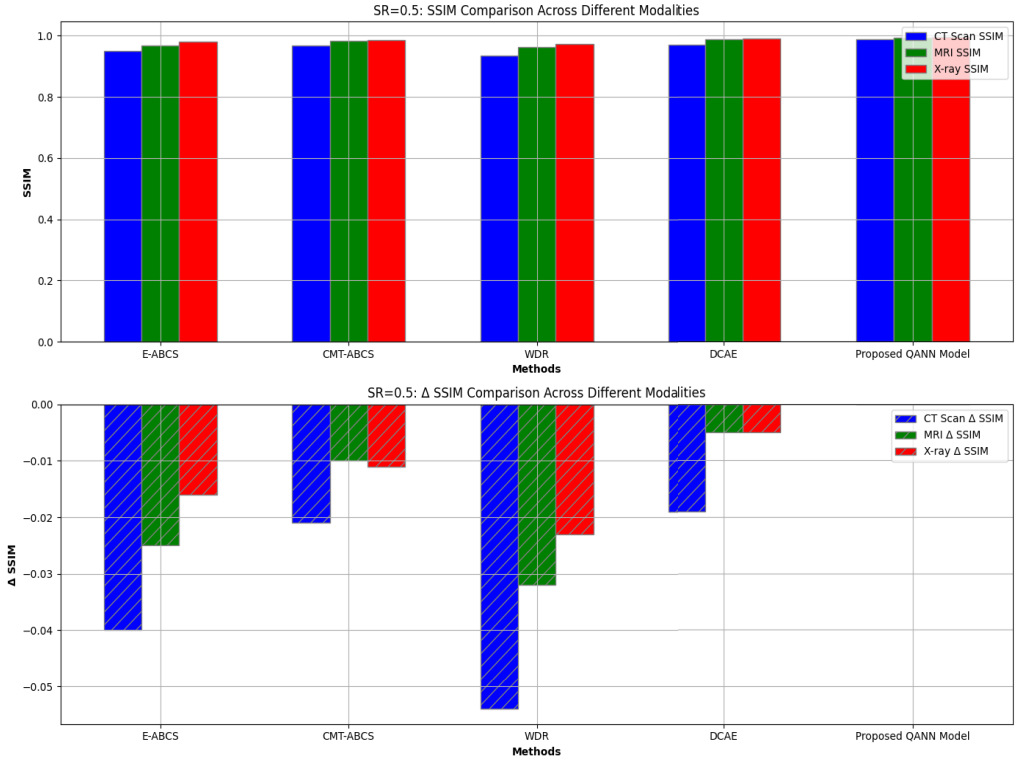

FIGURE 8. Analysis of SSIM and Delta SSIM in SR=0.5.

are 73.3%, 65.6%, and 63.7%, in that order. The space savings have, therefore, increased. In addition, the proposed technique takes less time to run the algorithm compared to other approaches shown in Fig 11. Table 8 shows the X-ray image's reduced size and space savings for different sampling rates. It also shows that the proposed QANN

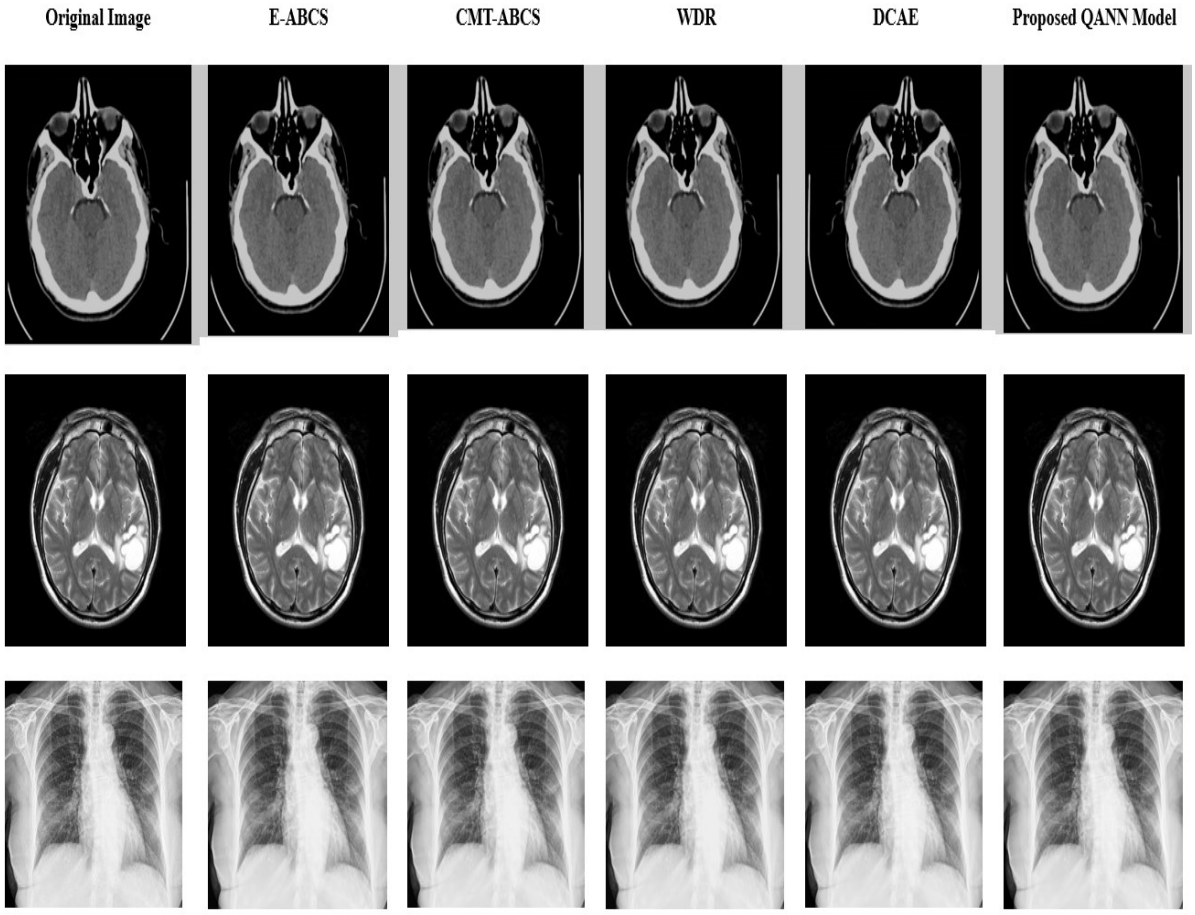

FIGURE 9. Sample Image compression of exiting methods and proposed method.

TABLE 6. CT-SCAN Image size and Space analysis.

CT-SCAN (Original Image Size= 77,900 bytes)						
Methods	Compressed image size (Bytes)			Space saving (%)		
SR	SR=0.1	SR=0.3	SR=0.5	SR=0.1	SR=0.3	SR=0.5
E-ABCS	34587.6	46584.2	51803.5	55.6	40.2	33.5
CMT-ABCS	25473.3	31082.1	32873.8	67.3	60.1	57.8
WDR	36690.9	47908.5	54452.1	52.9	38.5	30.1
DCAE	24460.6	29368.3	30848.4	68.6	62.3	60.4
Proposed QANN Model	21967.8	27732.4	29679.9	71.8	64.4	61.9

TABLE 7. MRI image size and Space analysis.

MRI SCAN (Original Image Size= 63,500 bytes)						
Methods	Compressed image size (Bytes)			Space saving (%)		
SR	SR=0.1	SR=0.3	SR=0.5	SR=0.1	SR=0.3	SR=0.5
E-ABCS	27750	36894	41021	56.3	41.9	35.4
CMT-ABCS	19749	23686	25337	68.9	62.7	60.1
WDR	28258	37846	42672	55.5	40.4	32.8
DCAE	18987	22352	23940	70.1	64.8	62.3
Proposed QANN Model	16955	21844	23051	73.3	65.6	63.7

TABLE 8. X-Ray Image size and Space analysis.

X-Ray (Original Image Size= 58,000 bytes)						
Methods	Compressed image size (Bytes)			Space saving (%)		
SR	SR=0.1	SR=0.3	SR=0.5	SR=0.1	SR=0.3	SR=0.5
E-ABCS	24882	32828	37004	57.1	43.4	36.2
CMT-ABCS	17458	21170	22388	69.9	63.5	61.4
WDR	25172	33756	38454	56.6	41.8	33.7
DCAE	16878	20126	21866	70.9	65.3	62.3
Proposed QANN Model	15022	19546	20764	74.1	66.3	64.2

model has achieved significant compression levels. For SR = 0.1, 0.3, and 0.5, the space savings are 74.1%, 66.3%, and 64.2%, in that order. Therefore, the space savings have increased. In addition, the proposed technique takes less time to run the algorithm compared to other approaches shown in Fig 12.

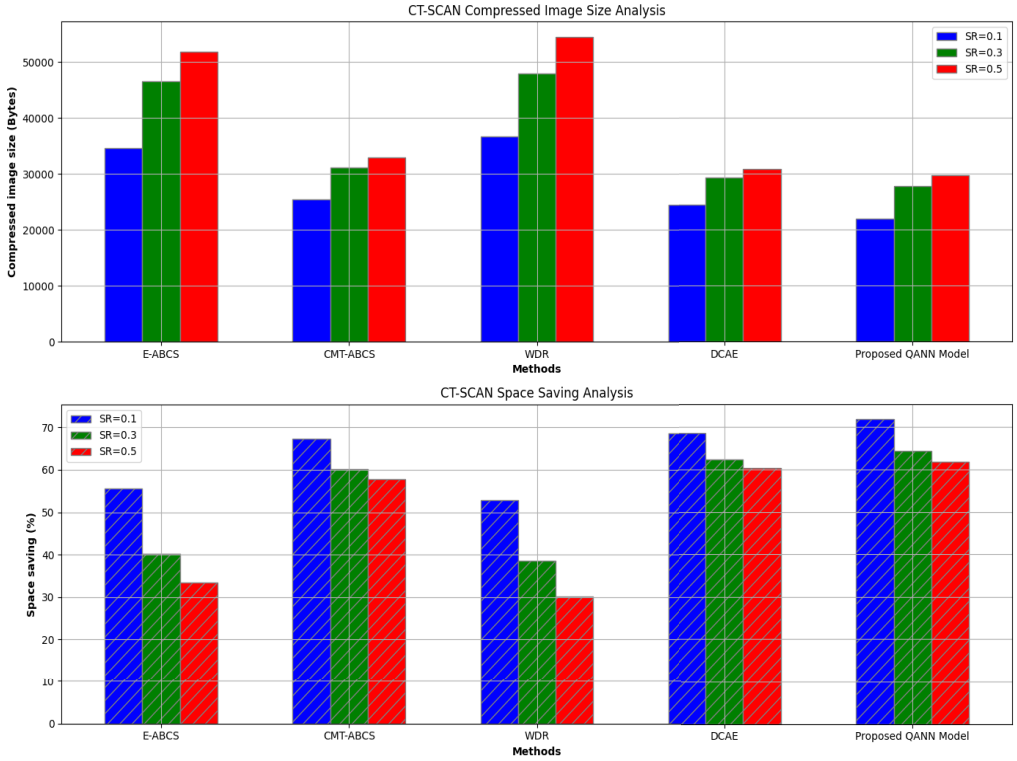

FIGURE 10. Analysis of CT-SCAN Image size and Space.

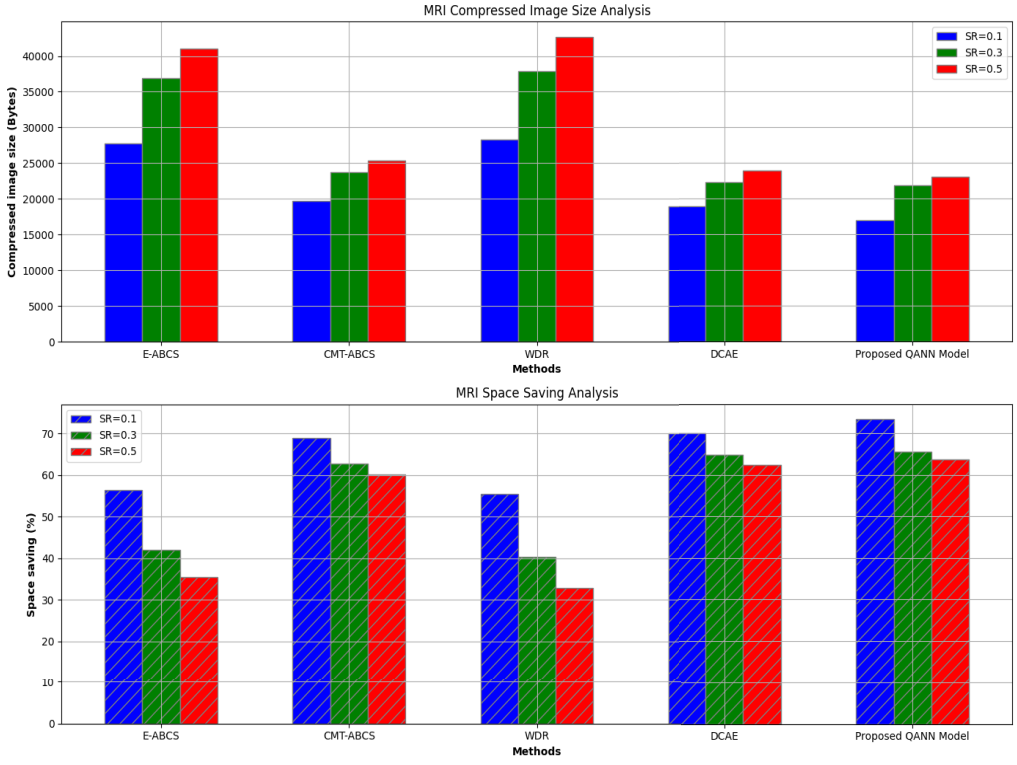

FIGURE 11. Analysis of MRI image size and space.

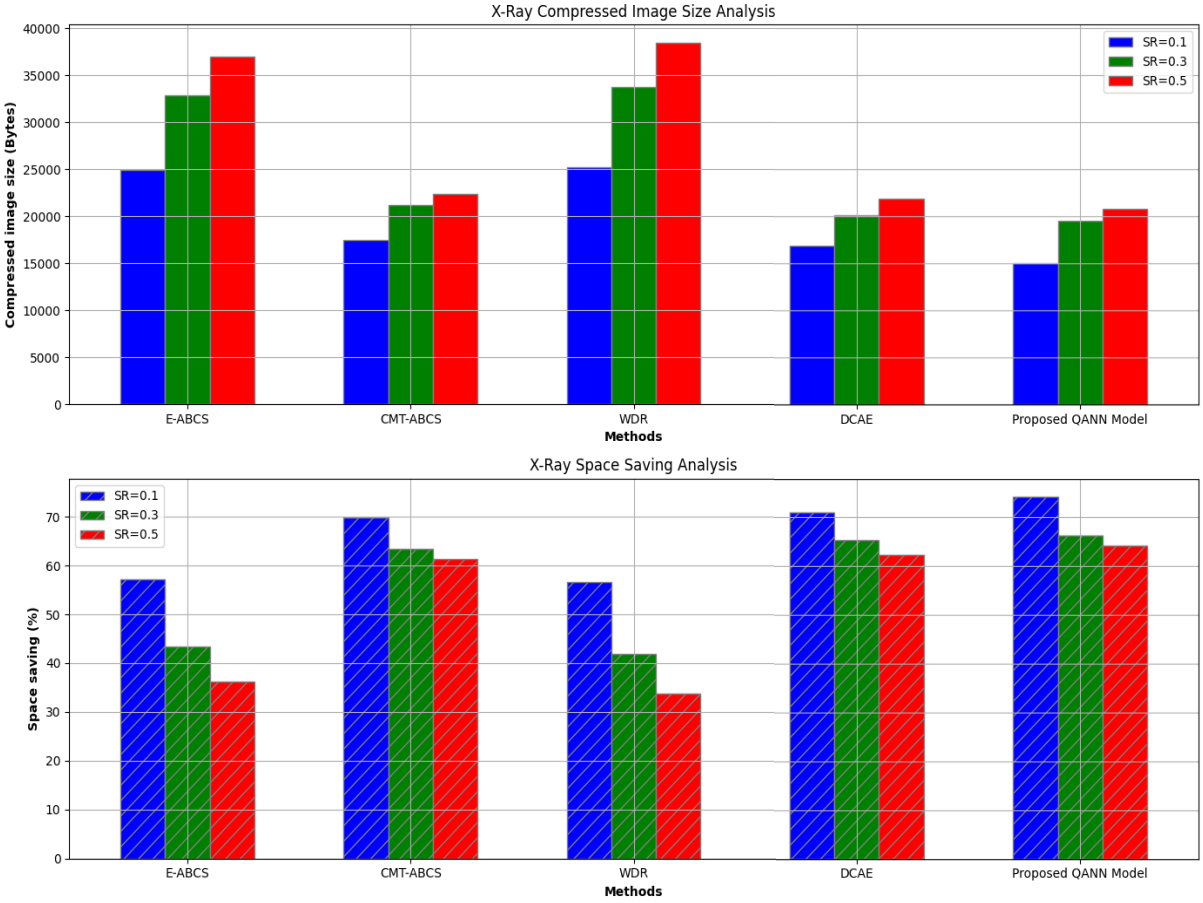

FIGURE 12. Analysis of X-Ray image size and space.

V. CONCLUSION

Using the QANN model, this study investigated the effectiveness of applying quantum computing techniques to improve the compression of medical image data. We presented a QANN model that combines quantum feature extraction with traditional neural network topologies. The QANN model has shown impressive progress in accurately identifying scenarios using ideas from quantum physics. The SSIM and PSNR are improved by the proposed QANN model. For MRI (73.3%), X-ray (74.1%), and CT-SCAN (71.8%), the image size is reduced using quantum technology to save space. It is essential to understand that each model has its advantages and disadvantages, and the selection process should be tailored to the particular characteristics of the dataset and problem domain. Although our results are encouraging, it is essential to understand the limitations of our research. Scalability issues, hardware constraints, and algorithm complexity are the main obstacles to the widespread implementation of quantum computing techniques in practical settings. Future research should focus on developing hybrid quantum-classical computing techniques, improving algorithms, and advancing quantum hardware. In addition to working with medical images, our proposed QANN model will need to be fine-tuned in the future so that it can be used with other videos and photos unrelated to medicine.

REFERENCES

[1] H. Yuxuan, D. Yining, R. Zhong, T. Yubo, and C. Wei, "Machine learning methods in medical image compression," *J. Comput.-Aided Des. Comput. Graph.*, vol. 33, no. 8, pp. 1151–1160, Aug. 20, 2021.

[2] Y. Zhang and Q. Ni, "Recent advances in quantum machine learning," *Quantum Eng.*, vol. 2, no. 1, p. e34, Mar. 2020.

[3] A. Abbas, D. Sutter, C. Zoufal, A. Lucchi, A. Figalli, and S. Woerner, "The power of quantum neural networks," *Nature Comput. Sci.*, vol. 6, pp. 403–412, Jun. 2021.

[4] S. K. Jeswal and S. Chakraverty, "Recent developments and applications in quantum neural network: A review," *Arch. Comput. Methods Eng.*, vol. 26, no. 4, pp. 793–807, Sep. 2019.

[5] Y.-Y. Chen, "Medical image compression using DCT-based subband decomposition and modified SPIHT data organization," *Int. J. Med. Informat.*, vol. 76, no. 10, pp. 717–725, Oct. 2007.

[6] A. Delilbasic, B. Le Saux, M. Riedel, K. Michielsen, and G. Cavallaro, "A single-step multiclass SVM based on quantum annealing for remote sensing data classification," *IEEE J. Sel. Topics Appl. Earth Observ. Remote Sens.*, vol. 17, pp. 1434–1445, 2024.

[7] A. K. K. Don and I. Khalil, "Q-SupCon: Quantum-enhanced supervised contrastive learning architecture within the representation learning framework," *ACM Trans. Quantum Comput.*, vol. 6, no. 1, pp. 1–24, Mar. 2025.

[8] S. Prabhu, S. Gupta, G. M. Prabhu, A. V. Dhanuka, and K. V. Bhat, "QuCardio: Application of quantum machine learning for detection of cardiovascular diseases," *IEEE Access*, vol. 11, pp. 136122–136135, 2023.

[9] M. H. Hassanshahi, M. Jastrzebski, S. Malik, and O. Lahav, "A quantum-enhanced support vector machine for galaxy classification," *RAS Techn. Instrum.*, vol. 2, no. 1, pp. 752–759, Jan. 2023.

[10] M. Y. Arafath and A. N. Kumar, "Quantum computing based neural networks for anomaly classification in real-time surveillance videos," *Comput. Syst. Sci. Eng.*, vol. 46, no. 2, pp. 2489–2508, 2023.

[11] G. Park, J. Huh, and D. K. Park, "Variational quantum one-class classifier," *Mach. Learn., Sci. Technol.*, vol. 4, no. 1, Mar. 2023, Art. no. 015006.

[12] Z. Xu, Y. Hu, T. Yang, P. Cai, K. Shen, B. Lv, S. Chen, J. Wang, Y. Zhu, Z. Wu, and Y. Dai, "Parallel structure of hybrid quantum-classical neural networks for image classification," *Res. Square*, Apr. 2024. [Online]. Available: https://doi.org/10.21203/rs.3.rs-4230145/v1

[13] J. Preskill, "Quantum computing in the NISQ era and beyond," *Quantum*, vol. 2, p. 79, Aug. 2018.

[14] N. M. De Oliveira, L. P. De Albuquerque, W. R. De Oliveira, T. B. Ludermir, and A. J. Da Silva, "Quantum one-class classification with a distance-based classifier," in *Proc. Int. Joint Conf. Neural Netw. (IJCNN)*, Jul. 2021, pp. 1–7.

[15] O. P. Patel and A. Tiwari, "Quantum inspired binary neural network algorithm," in *Proc. Int. Conf. Inf. Technol.*, Dec. 2014, pp. 270–274.

[16] K.-C. Chen, X. Xu, H. Makhanov, H.-H. Chung, and C.-Y. Liu, "Quantum-enhanced support vector machine for large-scale stellar classification with GPU acceleration," 2023, *arXiv:2311.12328*.

[17] M. Benedetti, J. Realpe-Gómez, and A. Perdomo-Ortiz, "Quantum-assisted Helmholtz machines: A quantum–classical deep learning framework for industrial datasets in near-term devices," *Quantum Sci. Technol.*, vol. 3, no. 3, Jul. 2018, Art. no. 034007.

[18] K. Mitarai, M. Negoro, M. Kitagawa, and K. Fujii, "Quantum circuit learning," *Phys. Rev. A, Gen. Phys.*, vol. 98, no. 3, 2018, Art. no. 032309.

[19] S. S. Alotaibi, H. A. Mengash, S. Dhahbi, S. Alazwari, R. Marzouk, M. A. Alkhonaini, A. Mohamed, and A M. Hilal, "Quantum-enhanced machine learning algorithms for heart disease prediction," *Hum.-Centric Comput. Inf. Sci.*, vol. 13, p. 41, Apr. 2023.

[20] M. Mazher, A. Qayyum, M. A. Khan, S. Niederer, M. Mokayef, and C. S. Hassan, "Hybrid classical and quantum deep learning models for medical image classification," in *Proc. Int. Conf. Artif. Life Robot. (ICAROB)*, 2024, pp. 222–226.

[21] Y. Dang, N. Jiang, H. Hu, Z. Ji, and W. Zhang, "Image classification based on quantum K-nearest-neighbor algorithm," *Quantum Inf. Process.*, vol. 17, no. 9, pp. 1–8, Sep. 2018.

[22] T. Villmann, A. Engelsberger, J. Ravichandran, A. Villmann, and M. Kaden, "Quantum-inspired learning vector quantizers for prototype-based classification: Confidential: For personal use only—Submitted to neural networks and applications 5/2020," *Neural Comput. Appl.*, vol. 34, no. 1, pp. 79–88, Nov. 2022.

[23] O. P. Patel, N. Bharill, A. Tiwari, and M. Prasad, "A novel quantum-inspired fuzzy based neural network for data classification," *IEEE Trans. Emerg. Topics Comput.*, vol. 9, no. 2, pp. 1031–1044, Apr. 2021.

[24] M. Nivelkar and S. G. Bhirud, "Optimized machine learning: Training and classification performance using quantum computing," in *Proc. IEEE 6th Int. Conf. Comput., Commun. Autom. (ICCCA)*, Dec. 2021, pp. 8–13.

[25] S. DiAdamo, C. O'Meara, G. Cortiana, and J. Bernabé-Moreno, "Practical quantum K-means clustering: Performance analysis and applications in energy grid classification," *IEEE Trans. Quantum Eng.*, vol. 3, pp. 1–16, 2022.

[26] Y. Zhang, D. Song, X. Li, P. Zhang, P. Wang, L. Rong, G. Yu, and B. Wang, "A quantum-like multimodal network framework for modeling interaction dynamics in multiparty conversational sentiment analysis," *Inf. Fusion*, vol. 62, pp. 14–31, Oct. 2020.

[27] B. Ahuja and R. Doriya, "An unsupervised learning approach for visual data compression with chaotic encryption," in *Proc. 4th Int. Conf. Electr., Comput. Commun. Technol. (ICECCT)*, Sep. 2021, pp. 1–4, doi: 10.1109/ICECCT52121.2021.9616827.

[28] A. Thakker, N. Namboodiri, R. Mody, R. Tasgaonkar, and M. Kambli, "Lossy image compression—A comparison between wavelet transform, principal component analysis, K-means and autoencoders," in *Proc. 5th Int. Conf. Adv. Sci. Technol. (ICAST)*, Dec. 2022, pp. 569–576, doi: 10.1109/ICAST55766.2022.10039613.

[29] P. Chakraborty and T. Chandrapragasam, "Extended applications of compressed sensing algorithm in biomedical signal and image compression," *J. Inst. Engineers India, B*, vol. 103, no. 1, pp. 83–91, Feb. 2022, doi: 10.1007/s40031-021-00592-8.

[30] S. S. Parikh, D. Ruiz, H. Kalva, G. Fernández-Escribano, and V. Adzic, "High bit-depth medical image compression with HEVC," *IEEE J. Biomed. Health Informat.*, vol. 22, no. 2, pp. 552–560, Mar. 2018, doi: 10.1109/JBHI.2017.2660482.

[31] S. Liu, W. Bai, N. Zeng, and S. Wang, "A fast fractal based compression for MRI images," *IEEE Access*, vol. 7, pp. 62412–62420, 2019, doi: 10.1109/ACCESS.2019.2916934.

[32] A. Sengupta and M. Rathor, "Structural obfuscation and crypto-steganography-based secured JPEG compression hardware for medical imaging systems," *IEEE Access*, vol. 8, pp. 6543–6565, 2020, doi: 10.1109/ACCESS.2019.2963711.

[33] D. Xue, H. Ma, L. Li, D. Liu, and Z. Xiong, "AiWave: Volumetric image compression with 3-D trained affine wavelet-like transform," *IEEE Trans. Med. Imag.*, vol. 42, no. 3, pp. 606–618, Mar. 2023, doi: 10.1109/TMI.2022.3212780.

[34] M. C. H. Zerva, V. Christou, N. Giannakeas, A. T. Tzallas, and L. P. Kondi, "An improved medical image compression method based on wavelet difference reduction," *IEEE Access*, vol. 11, pp. 18026–18037, 2023, doi: 10.1109/ACCESS.2023.3246948.

[35] Z. Li, A. Ramos, Z. Li, M. L. Osborn, W. Zaid, X. Li, Y. Li, and J. Xu, "Nearly-lossless-to-lossy medical image compression by the optimized JPEGXT and JPEG algorithms through the anatomical regions of interest," *Biomed. Signal Process. Control*, vol. 83, May 2023, Art. no. 104711.

[36] P. N. T. Ammah and E. Owusu, "Robust medical image compression based on wavelet transform and vector quantization," *Informat. Med. Unlocked*, vol. 15, Apr. 2019, Art. no. 100183.

[37] B. Lalithambigai and S. Chitra, "A hybrid adaptive block based compressive sensing in video for IoMT applications," *Wireless Netw.*, vol. 10, pp. 1–10, Jan. 2022, doi: 10.1007/s11276-021-02847-0.

[38] R. Monika, D. Samiappan, and R. Kumar, "Underwater image compression using energy based adaptive block compressive sensing for IoUT applications," *Vis. Comput.*, vol. 37, no. 6, pp. 1499–1515, Jun. 2021.

[39] R. Monika and S. Dhanalakshmi, "An efficient medical image compression technique for telemedicine systems," *Biomed. Signal Process. Control*, vol. 80, Feb. 2023, Art. no. 104404.

[40] A. Fettah, R. Menassel, A. Gattal, and A. Gattal, "Convolutional autoencoder-based medical image compression using a novel annotated medical X-ray imaging dataset," *Biomed. Signal Process. Control*, vol. 94, Aug. 2024, Art. no. 106238.

[41] *CT and MRI Dataset*. Accessed: Dec. 20, 2024. [Online]. Available: https://www.kaggle.com/datasets/darren2020/ct-to-mri-cgan

[42] A. Haghanifar, M. M. Majdabadi, and S. Ko, 2020, "COVID-19 chest X-ray image repository," Figshare, doi: 10.6084/m9.figshare.12580328.v3.

[43] N. Jiang, X. Lu, H. Hu, Y. Dang, and Y. Cai, "A novel quantum image compression method based on JPEG," *Int. J. Theor. Phys.*, vol. 57, no. 3, pp. 611–636, Mar. 2018.

[44] S. K. Deb and W. D. Pan, "Quantum image compression: Fundamentals, algorithms, and advances," *Computers*, vol. 13, no. 8, p. 185, Jul. 2024.

[45] S. Du, Y. Yan, and Y. Ma, "Quantum-accelerated fractal image compression: An interdisciplinary approach," *IEEE Signal Process. Lett.*, vol. 22, no. 4, pp. 499–503, Apr. 2015.

BALASUBRAMANI SUBBIYAN received the B.Tech. degree in information technology and the M.E. degree in computer science and engineering from Anna University, Chennai, India, in 2012 and 2015, respectively, and the Ph.D. degree in computer science engineering from the Hindustan Institute of Technology and Science, Chennai, in 2023. He is currently an Assistant Professor with the Computer Science and Engineering Department, Koneru Lakshmaiah Education Foundation, Vijayawada. He has published several research articles in international journals and conferences. As a reviewer, he conducts peer reviews of research articles for the prestigious IEEE, Elsevier, and Springer journals. His research interests include information security, the IoT security, distributed computing, machine learning, and blockchain technology.

RENJITH PRABHAVATHI NEELAKANDAN received the B.Tech. degree in information technology and the Master of Engineering degree in computer science and engineering from Anna University, in 2005 and 2010, respectively, and the Ph.D. degree in computer science and engineering from Anna University, Chennai, India, specializing in the area of security in wireless sensor networks. He is currently an Assistant Professor SG2 with the Computer Science and Engineering Department, Vellore Institute of Technology, Chennai. He has demonstrated his expertise through the publication of numerous papers and the filing of two patents in these domains. In addition to his research pursuits, he is a dedicated educator who imparts knowledge on several subjects, including *Computer Networks*, *Theory of Computation*, *Advanced Programming with Python*, *Wireless Sensor Networks*, and *Internet of Things*. His comprehensive understanding and teaching abilities make him an invaluable asset to any academic conference in the field of sensors and sensing technology. His research interests include various aspects of wireless sensor networks (WSNs), big data analytics, mobile ad hoc networks (MANETs), vehicular ad hoc networks (VANETs), network security, and quality of service (QoS).

KAVISANKAR LEELASANKAR is currently an Associate Professor with the SRM Institute of Science and Technology, Kattankulathur, Tamil Nadu. He was previously a Research Associate with the "Collaborated Directed Basic Research Smart and Secure Environment" (CDBR-SSE). He is a Postdoctoral Fellow with IIITA working on the C3ihub IHUBNF, IIT Kanpur sponsored "IoT Security-Development of Security Audit Framework for Secure IoT Network" project. He is the Smart and Secure Environment Research Consortium, which connects eight Tamil Nadu institutions, and is funded by the National Technical Research Organisation (NTRO), New Delhi. He is with the PSG College of Technology Coimbatore, Pondicherry University, Thiagarajar College of Engineering, Madurai, Madurai Kamaraj University Madurai, IIT Madras, NIT Tiruchirapalli, and Pondicherry University, Guindy, Anna University, Chennai are among the institutions. This connection is made possible by MPLS-VPN. The project is valued at nine lakhs for more than five years, from 2007 to 2012. During this time, several cybersecurity flaws are being addressed. Users investigate "Intrusion Detection Prevention" to build a framework for detecting and mitigating multi-vector DDoS attacks. He oversaw the study while serving as the Dean of CEG, Anna University. He is interested in quantum computing, computer forensics, the Internet of Things, cyber security, and network security.

RAJKUMAR RAJAVEL received the Ph.D. degree from the Anna Centenary Research Fellow, Department of Information Science and Technology, Anna University, Chennai, India, in August 2016. He is currently an Associate Professor with the Department of Computer Science and Engineering, Christ University, Bengaluru, India. He has published 11 research publications in the reputed SCI journals. His research interests include cloud computing, quantum computing, big data analytics, and the Internet of Things.

MUTHUKUMARAN MALARVEL (Senior Member, IEEE) received the Ph.D. degree in digital image processing from IGCAR, India. He is currently a Professor with the Department of Computer Science and Engineering, Aarupadai Veedu Institute of Technology, Vinayaga Mission's Research Foundation (deemed to be University), Chennai, India. He has more than 20 years of experience which includes the IT industry, teaching, and rich research experience. He received a Senior Research Fellowship (SRF) under the collaborative funded project of the Board of Research in Nuclear Sciences (BRNS), Government of India, and IGCAR. He published more than 30 research articles, including nine SCI-indexed articles. He edited three books in Taylor and Francis and John Wiley publications, and he is an editor and a reviewer of reputed journals, such as IEEE Access, *Soft Computing*, and *Journal of Intelligence and Fuzzy Systems*. He filed five patents in intellectual property in India and one international patent, and received two national and one international patent grant. His research interests include digital image processing, machine vision systems, image statistical analysis and feature extraction, pattern recognition, and machine learning techniques.

ACHYUT SHANKAR received the Ph.D. degree in computer science and engineering majoring in wireless sensor networks from VIT University, Vellore, India. He is currently an Associate Professor with Bennett University, Greater Noida, India. He was with the University of Warwick, U.K., from November 2022 to November 2024. He is also an associated with the University of Johannesburg, South Africa, as a Visiting Associate Professor and Maryam Abacha American University, Nigeria, as an Honorary Adjunct Faculty. He was with Birkbeck University, London from January 2022 to May 2022, for his research work. He has published more than 200 research papers in reputed international conferences and journals of which 160 papers are in SCIE journals. His research interests include electronic vehicle, wireless sensor networks, the Internet of Things, blockchain, and machine learning. He is a member of ACM. He has received a research award for excellence in research, in 2016 and 2017. He had organized many special sessions with Scopus Indexed International Conferences worldwide, proceedings of which were published by Springer, IEEE, and Elsevier. He received the Young Scientist Award, in 2020 for excellence in research. He is an Associate Editor and a Guest Editor for a few SCI journals for the last four years, and other prestigious conferences.